bioRxiv preprint doi: https://doi.org/10.1101/2022.06.07.495149; this version posted June 8, 2022. The copyright holder for this preprint (which was not certified by peer review) is the author/funder, who has granted bioRxiv a license to display the preprint in perpetuity. It is made available under aCC-BY-ND 4.0 International license.

SARS-CoV-2 spike protein induces long-term TLR4-mediated synapse and cognitive loss recapitulating Post-COVID syndrome

Fabricia L. Fontes-Dantas[1,2*]; Gabriel G. Fernandes[1*]; Elisa G. Gutman[3,4*], Emanuelle V. De Lima[1], Leticia S. Antonio[1], Mariana B. Hammerle[4], Hannah P. Mota-Araujo[1], Lilian C. Colodeti[1], Suzana M. B. Araújo[1], Talita N. da Silva [1], Larissa A. Duarte[3,4], Andreza L. Salvio[3], Karina L. Pires[5]; Luciane A. A. Leon[6], Claudia Cristina F. Vasconcelos[5], Luciana Romão[7], Luiz Eduardo B. Savio[8], Jerson L. Silva[9], Robson da Costa[1], Julia R. Clarke[7], Andrea T. Da Poian[9#], Soniza V. Alves-Leon[3,10#], Giselle F. Passos[1#]; Claudia P. Figueiredo[1#]

[1] School of Pharmacy, Federal University of Rio de Janeiro, Rio de Janeiro, RJ, Brazil.

[2] Department of Pharmacology, Institute of Biology, Rio de Janeiro State University, Rio de Janeiro, RJ, Brazil

[3] Translational Neuroscience Laboratory (LabNet), Post-Graduate Program in Neurology, Federal University of Rio de Janeiro State, RJ, Brazil.

[4] Clinical Medicine post-graduation program, Federal University of Rio de Janeiro, Rio de Janeiro, RJ, Brazil

[5] Neurology Department of Federal University of the State of Rio de Janeiro (UNIRIO), Rio de Janeiro, Brazil.

[6] Laboratório de Desenvolvimento Tecnológico em Virologia. IOC/FIOCRUZ, Rio de Janeiro, Brasil.

[7] Institute of Biomedical Sciences, Federal University of Rio de Janeiro, Rio de Janeiro, RJ 21944-590, Brazil.

[8] Institute of Biophysics Carlos Chagas Filho, Federal University of Rio de Janeiro, Rio de Janeiro, RJ 21944-590, Brazil.

[9] Institute of Medical Biochemistry Leopoldo de Meis, Federal University of Rio de Janeiro, Rio de Janeiro, RJ 21944-590, Brazil.

[10] Division of Neurology, Hospital Clementino Fraga Filho, Federal University of Rio de Janeiro, Rio de Janeiro, RJ, Brazil

These authors contributed equally: Fabricia L. Fontes-Dantas, Gabriel Gripp Fernandes; Elisa G. Gutman.

Correspondence and requests for materials should be addressed to A.T.D.P. (email: dapoian@bioqmed.ufrj.br), S.V.A.L (email: sonizavieiraalvesleon@gmail.com), G.P.F. (email: gfazzioni@yahoo.com.br) or to C.P.F. (email: claudia@pharma.ufrj.br).

bioRxiv preprint doi: https://doi.org/10.1101/2022.06.07.495149; this version posted June 8, 2022. The copyright holder for this preprint (which was not certified by peer review) is the author/funder, who has granted bioRxiv a license to display the preprint in perpetuity. It is made available under aCC-BY-ND 4.0 International license.

Summary

COVID-19 pandemic affected the global population in an unprecedented scale, with long-term consequences of SARS-CoV-2 infection now emerging as a serious concern. Cognitive dysfunction is often reported in post-COVID patients, but its underlying mechanisms remain unknown. Here we demonstrated that brain exposure to SARS-CoV-2 spike (S) protein through its infusion into the lateral ventricle of adult mice induced late cognitive impairment, hippocampal synapse loss, and microglial engulfment of presynaptic terminals. Additionally, TLR4 blockage prevented S-associated detrimental effects on memory in mice and *TLR4* single nucleotide polymorphism (SNP) rs10759931 was associated with late cognitive outcome in mild COVID-19-recovered patients. Collectively, these findings indicate that S protein directly impacts the brain and identify TLR4 as a key target to prevent cognitive dysfunction. To our knowledge, this is the first animal model that recapitulates post-COVID cognitive impairment, opening new avenues for developing new strategies to prevent or treat the neurological outcomes of COVID-19.

Keywords: COVID-19, Spike protein, Cognitive dysfunction, synapse loss, TLR4, single nucleotide polymorphism.

bioRxiv preprint doi: https://doi.org/10.1101/2022.06.07.495149; this version posted June 8, 2022. The copyright holder for this preprint (which was not certified by peer review) is the author/funder, who has granted bioRxiv a license to display the preprint in perpetuity. It is made available under aCC-BY-ND 4.0 International license.

Introduction

Severe acute respiratory syndrome coronavirus 2 (SARS-CoV-2) is considered a respiratory pathogen, but the impact of the infection on extrapulmonary tissues is of high concern. Coronavirus disease 2019 (COVID-19) is associated with unpredictable and variable outcomes, and while most patients show a positive recovery after the acute stages, others experience a myriad of acute and long term neurological dysfunctions(Abdel-Mannan et al., 2020). Cognitive impairment is a well-characterized feature of the post-COVID syndrome, referred to as “long COVID” or brain fog(Blomberg et al., 2021). Mounting evidence suggest that COVID-induced neurological symptoms are mediated by multiple mechanisms, including brain hypoxia and systemic inflammation even in patients with mild symptoms(Almeria et al., 2020; Alonso-Lana et al., 2020). Despite some findings indicating that SARS-CoV-2 can reach and directly impact the brain, others indicate that the virus can rarely cross the blood-brain-barrier (BBB)(Edén et al., 2021; Farhadian et al., 2020). Nevertheless, whether brain presence of SARS-CoV-2 viral particles and/or its products is a crucial event for the development of cognitive impairment in post-COVID patients remains unknown.

SARS-CoV-2 spike (S) protein plays a pivotal role in COVID-19 pathogenesis and is the main target for vaccine development. This viral surface protein is a homotrimer composed of two functional domains, also known as subunits (S1 and S2), as they are generated by proteolytic cleavage of S protein after virus binding to enzyme 2 angiotensin-converting (ACE2), which mediates cell entry(Walls et al., 2020). During SARS-CoV-2 infection, cells produce and release variable amounts of viral particles and proteins, including the S

bioRxiv preprint doi: https://doi.org/10.1101/2022.06.07.495149; this version posted June 8, 2022. The copyright holder for this preprint (which was not certified by peer review) is the author/funder, who has granted bioRxiv a license to display the preprint in perpetuity. It is made available under aCC-BY-ND 4.0 International license.

protein(Walls et al., 2020; Wang et al., 2021). The S1 was shown to cross the BBB, reaching different memory-related regions of the brain in a mouse model of SARS-CoV-2 infection(Rhea et al., 2020). Inflammation and increased BBB permeability were also shown in *in vitro* models of S1 exposure(Buzhdygan et al., 2020). Likewise, the protein was detected in the central nervous system (CNS) of COVID-19 patients, irrespective of viral RNA detection(Matschke et al., 2020; Yang et al., 2021). In addition, increased levels of proinflammatory cytokines and brain gliosis have been reported in severe COVID-19 patients(Martin et al., 2022; Pilotto et al., 2021). Nonetheless, proof concerning the acute and chronic impact of S protein on COVID-19 brain dysfunction and its underlying mechanisms are still lacking.

Most experimental studies investigating the effects of SARS-CoV-2 have focused on acute infection, especially on peripheral tissues. Few studies have used experimental models to evaluate the possible mechanism of post-COVID syndrome. Here, we developed a mouse model of intracerebroventricular (icv) of S exposure to understand the role of this protein in late cognitive impairment after viral infection. Here, we infused S protein in the brains of mice and performed a long-term (45 days) follow-up of the behavioral, neuropathological, and molecular consequences. We report late cognitive impairment, synapse loss, and microglial engulfment of presynaptic terminals after icv infusion of S protein. Early TLR4 blockage prevented S-associated detrimental effects on memory. We also demonstrated that the single nucleotide polymorphism (SNP) rs10759931, linked with increased TLR4 expression is associated with long-term cognitive impairment in mild COVID-19-recovered patients. Collectively, these findings show that S protein impacts the mouse CNS, independent of virus infection, and

bioRxiv preprint doi: https://doi.org/10.1101/2022.06.07.495149; this version posted June 8, 2022. The copyright holder for this preprint (which was not certified by peer review) is the author/funder, who has granted bioRxiv a license to display the preprint in perpetuity. It is made available under aCC-BY-ND 4.0 International license.

identify TLR4 as a key mediator and interesting target to investigate the long-term cognitive dysfunction both in humans and rodents.

Results

SARS-CoV-2 spike protein induces long-term cognitive impairment and synapse loss in mice

COVID-19 is associated with long-term cognitive dysfunction(Blomberg et al., 2021). To evaluate whether SARS-CoV-2 spike protein induces behavioral changes, we infused the protein into mouse brains through icv route. The experiments were performed in two different timeframes: “early and “late” phases, corresponding to assessments performed within the first 7 days and between 30 and 45 days after S protein infusion, respectively (Fig. 1A). Animals were submitted to behavioral tests or culled to collect brain or blood samples at different time points after infusion (Fig. 1A). To evaluate the effect of S protein infusion on declarative memory, mice were evaluated using the novel object recognition (NOR) test(Figueiredo et al., 2019). Vehicle-infused mice (Veh) were able to perform the NOR task as demonstrated by a longer exploration of the novel object over the familiar one (Fig. 1B-D, white bars). The S protein had no impact on memory function in the early phase after brain infusion (Fig. 1B, gray bars), while in later time points infused mice failed to recognize the novel object (Fig. 1C-D, black bars). In order to rule out the possibility that changes in motivation, motor function and/or anxiety levels eventually induced by S protein infusion were influencing NOR interpretation, mice were submitted to the rotarod and open field tests. Both S protein- and Veh-infused groups showed similar innate preferences for the objects in the NOR memory test (Supplementary Fig.

bioRxiv preprint doi: https://doi.org/10.1101/2022.06.07.495149; this version posted June 8, 2022. The copyright holder for this preprint (which was not certified by peer review) is the author/funder, who has granted bioRxiv a license to display the preprint in perpetuity. It is made available under aCC-BY-ND 4.0 International license.

1A-C), similar motivation towards object exploration in the NOR sessions (Supplementary Fig. 1D-F) and performed similarly in the rotarod (Fig. 1E) and open field tests (Fig. 1F-G).

Late cognitive dysfunction induced by S protein infusion was confirmed by the Morris Water Maze (MWM) test, a task widely used to assess spatial memory in rodents(Vorhees and Williams, 2006). Mice infused with S protein showed higher latency time to find the submerged platform in sessions 3 and 4 of MWM training, when compared to control mice (Fig. 1H). Also, S protein-infused mice showed reduced memory retention, as indicated by the decreased time spent by these animals in the target quadrant during the probe trial (Fig. 1I). No difference in the swimming speed (Supplementary Fig. 1G) or distance traveled (Supplementary Fig. 1H) were found between groups during the test session.

The role of autoantibodies or autoimmune mechanisms in COVID-19 pathology is still controversial(Dotan et al., 2021). To evaluate whether an anti-S immune response was involved in the cognitive impairment observed in our model, we assessed the serum levels of anti-S protein antibodies in the mice inoculated with S protein either by subcutaneous or by icv. routes. As expected, peripheral S protein injection increased serum levels of anti-S antibodies (Supplementary Fig. 1I). On the other hand, no stimulation of anti-S antibody production was observed in icv. infused animals (Supplementary Fig. 1J). Together, these findings show that the cognitive impairment induced by brain exposure of S protein is an event independent of anti-S antibodies.

Synapse loss is strongly correlated to the cognitive decline observed in neurodegenerative diseases(Hong et al., 2016). Thus, we next investigated whether S protein induces synapse damage in the mouse hippocampus, a brain

bioRxiv preprint doi: https://doi.org/10.1101/2022.06.07.495149; this version posted June 8, 2022. The copyright holder for this preprint (which was not certified by peer review) is the author/funder, who has granted bioRxiv a license to display the preprint in perpetuity. It is made available under aCC-BY-ND 4.0 International license.

region critical for memory consolidation. S protein-infused mice did not show changes in synaptic density at the early stages, as demonstrated by the similar immunostaining for synaptophysin (SYP) and Homer-1 (pre- and postsynaptic markers, respectively) compared with the control group (Fig. 1J-M). Equivalent results were also found for the colocalization of these synaptic markers, which indicates no changes in synaptic density (Fig. 1J-K, N). In contrast, decreased SYP immunostaining and synaptic puncta were observed longer periods after S protein infusion (Fig. 1O-S), indicating that spike-induced cognitive dysfunction (shown in Figs. 1D, H, I) displays temporal correlation with hippocampal synapse damage (Fig. 1O-S). Collectively, these data suggest that a single brain infusion of S protein induces late synaptic loss and cognitive dysfunction, mimicking the post-COVID syndrome (Almeria et al., 2020; Blomberg et al., 2021).

SARS-CoV-2 spike protein triggers late neuroinflammation in mice

Neurodegeneration associated with viral brain infections can be mediated either by direct neuronal injury or by neuroinflammation(Shives et al., 2017). To advance in the understanding of the genuine impact of SP on neurons, cultured primary cortical neurons were incubated with S protein for 24 h. Neuron exposure to S protein did not affect neuron morphology (Supplementary Fig. 2A-E), once the percent of pyknotic nuclei (Supplementary Fig. 2C), number of primary neurites (Supplementary Fig. 2D) and intensity of β3-tubulin immunostaining (Supplementary Fig. 2E) were similar for vehicle- and S protein-incubated neurons. Also, S protein incubation also had no effect on the neuronal synaptic density and puncta (Supplementary Fig. 2F-J), suggesting that neurons are not directly affected by S protein.

bioRxiv preprint doi: https://doi.org/10.1101/2022.06.07.495149; this version posted June 8, 2022. The copyright holder for this preprint (which was not certified by peer review) is the author/funder, who has granted bioRxiv a license to display the preprint in perpetuity. It is made available under aCC-BY-ND 4.0 International license.

Microglia is the primary innate immune cell of the brain and plays a critical role in neuroinflammation-induced cognitive dysfunction(Chen et al., 2019). To further understand the impact of spike protein on microglial activation, mouse microglia BV-2 cell lineages were incubated with S protein for 24h. We found that S protein stimulation increased Iba-1 immunoreactivity (Fig. 2A and Supplementary Fig. 2K-L) and upregulated TNF, INF-β and IL-6 expression (Fig. 2B-D), without affecting IL-1β and IFNAR2 (Fig. 2E-F). To evaluate the time course of the in vivo activation of microglia, we analyzed cellular features and cytokine production in our mouse model. We found that at the early stage after icv. injection of S protein neither changed the number and morphology of microglia (Fig. 2G-J) nor increased the levels of TNF-α, IL-1β, IL-6, INF-β and IFNAR1 (Fig. 2K-O). In contrast, the levels of IFNAR2 mRNA decreased significantly at the same time point after S protein infusion (Fig. 2P). Notably, assessments performed late after revealed an increased number of Iba-1-positive cells (Fig. 2Q-S) and a predominance of cells with ameboid morphology in the hippocampus (Fig. 2Q, R, T), suggestive of microglial cells in a reactive state. However, no differences in GFAP immunoreactivity were detected in S protein-infused mice when compared to the control group (Supplementary Fig. 3A-C). The level and/or expression of the proinflammatory cytokines TNF, IL-1β, IFNα and IFNβ (Fig. 2U-Y) and the receptor IFNAR2 (Fig. 2Z) were higher in the hippocampus of S protein brain infused mice at this time point. Hippocampal expression of IL-6 and IFN-ɣ cytokines and the receptor IFNAR1 were unaffected by S protein infusion (Supplementary Fig. 3D-F). Altogether, our results indicate that the cognitive impairment induced by S protein is accompanied by microglial activation and neuroinflammation.

bioRxiv preprint doi: https://doi.org/10.1101/2022.06.07.495149; this version posted June 8, 2022. The copyright holder for this preprint (which was not certified by peer review) is the author/funder, who has granted bioRxiv a license to display the preprint in perpetuity. It is made available under aCC-BY-ND 4.0 International license.

SARS-CoV-2 spike protein induces C1q-mediated synaptic phagocytosis by microglia in mice

Synaptic phagocytosis (or synaptic pruning) by microglia was shown to underlie cognitive dysfunction in dementia and in viral encephalitis(Hong et al., 2016; Vasek et al., 2016). We therefore evaluated whether synaptic phagocytosis by microglia mediates S protein-induced synapse damage. Hippocampal three-dimensional image reconstructions of Iba-1-positive cells from S protein-infused mice showed increased SYP-positive terminals inside phagocytic cells (Fig. 3A-D). The complement component 1q (C1q) protein is known to be involved in the initial tagging of synapses, preceding synaptic engulfment by microglial cells(Stevens et al., 2007). Accordingly, we found that C1q was significantly upregulated in the brains of mice late (but not early) after S protein infusion (Fig. 3E, F). This finding led us to investigate whether or not the blockage of soluble C1q, using a neutralizing antibody, could restore cognitive function in S protein-infused mice. For this, the animals were treated by icv. route with a neutralizing C1q antibody immediately after S protein infusion and twice a week for 30 days (Fig. 3G). Remarkably, C1q blockage rescued memory impairment in S protein-infused mice (Fig. 3H), without any effect on locomotion (Fig. 3I) or exploration (Supplementary Fig. 4A, B). As seen for many viral encephalitis, these data suggest that C1q-mediated microglial phagocytosis underlie long-term cognitive dysfunction induced by S protein.

TLR-4 mediates cognitive dysfunction induced by SARS-CoV-2 spike protein

Recent findings have described that S protein induces toll-like receptor 4 (TLR4) activation in cultured immune cells(Zhao et al., 2021). Additionally, TLR4

bioRxiv preprint doi: https://doi.org/10.1101/2022.06.07.495149; this version posted June 8, 2022. The copyright holder for this preprint (which was not certified by peer review) is the author/funder, who has granted bioRxiv a license to display the preprint in perpetuity. It is made available under aCC-BY-ND 4.0 International license.

has been implicated in microglial activation and cognitive dysfunction in degenerative chronic disease of CNS like Alzheimer's disease(Miron et al., 2019). In agreement with these observations, despite no changes found in TLR4 expression levels at the early time point after S protein infusion (Fig. 4A), we found a late upregulation of TLR4 gene (Fig. 4B) in the hippocampus of infused mice that matches the late cognitive dysfunction (shown in Figs. 1C-D, H-I). To evaluate the role of TLR4 in spike-induced cognitive impairment we used either a pharmacological approach or a TLR4 knockout mouse model (TLR4$^{-/-}$). First, to investigate whether activation of TLR4 is an early event that could impact cognition later on, mice were treated with the TLR4 inhibitor TAK242 1h before S protein brain infusion and once a day for 7 days (Fig. 4C). Remarkably, early inhibition of TLR4 greatly prevented late memory dysfunction induced by S protein infusion in mice (Fig. 4D). Recent evidence has shown that high plasmatic levels of Neurofilament-light chain (NFL) are correlated with poor outcome in and COVID-19 patients(Edén et al., 2021; Pilotto et al., 2021; Sun et al., 2021). Then, we evaluated the NFL levels in plasma samples of control and S protein-infused mice, treated or not with TAK242 (Fig. 4F). Using transgenic mice, in the early phase after infusion, both WT and TLR4$^{-/-}$ mice learned the NOR task (Supplementary Fig. 4C). On the other hand, when evaluated at a late time point after protein infusion, WT mice had a poor performance in NOR test, while TLR4$^{-/-}$ animals were able to execute the task (Fig. 4G). Also, the absence of TLR4-mediated response in the TLR4$^{-/-}$ mice prevented the reduction of SYP-positive terminals inside phagocytic cells later after S protein infusion in comparison to WT mice (Fig. 4H-L). Consistent with the previous results, control experiments showed that genetic (Supplementary Fig. 4D-I) or pharmacological

bioRxiv preprint doi: https://doi.org/10.1101/2022.06.07.495149; this version posted June 8, 2022. The copyright holder for this preprint (which was not certified by peer review) is the author/funder, who has granted bioRxiv a license to display the preprint in perpetuity. It is made available under aCC-BY-ND 4.0 International license.

(Supplementary Fig. 4J-L) inhibition of TLR4 had no effect on locomotion or exploratory behavior. These data suggest that TLR4 activation mediates cognitive deficit and synaptic pruning induced by S protein in mice.

Importantly, the early treatment with TLR4 inhibitor prevented the late neuronal damage, indicating that the TLR4 pathway is central to induce neurodegeneration and long-term cognitive impairment in the present model.

Single nucleotide polymorphism within TLR4 gene is associated with increased risk of cognitive dysfunction after COVID-19

Several lines of evidence have suggested that polymorphisms in TLR4 is a risk factor for developing inflammatory diseases, including sporadic Alzheimer's disease(Miron et al., 2019; Yu et al., 2012). Thus, we sought to extend our findings by investigating whether there is an association between TLR4 gene variants and cognitive outcomes in COVID-19 patients. For this, 86 individuals with confirmed COVID-19 diagnosis, mostly with mild disease, were included in the study sample (Fig. 4M). Characteristics of the sample are displayed in Supplementary Table 1. Cognition was assessed using the Symbol Digit Modalities Test (SDMT) from 1 to 16 months after the onset of COVID-19 acute symptoms (Mean: 6.85 months). Of interest, nearly half of the patients evaluated (40; 46.51%) presented an important degree of post-COVID-19 cognitive impairment (Table 1). Genotyping analysis for two different SNPs (rs10759931 and rs2737190) was performed in all studied subjects. Individuals carrying the *TLR4*-2604G>A (rs10759931) GG homozygous genotype demonstrated a significantly higher risk for developing cognitive impairment following SARS-CoV-2 infection (*p*-value = 0.0234; OR= 1.91), while the GA genotype was associated

bioRxiv preprint doi: https://doi.org/10.1101/2022.06.07.495149; this version posted June 8, 2022. The copyright holder for this preprint (which was not certified by peer review) is the author/funder, who has granted bioRxiv a license to display the preprint in perpetuity. It is made available under aCC-BY-ND 4.0 International license.

with a decreased risk (*p*-value = 0.0209; OR= 0.50) (Fig. 4N and Table 1). Conversely, none of the *TLR4-2272A>G* (rs2737190) genotype variations were associated with increased susceptibility to post-COVID-19 cognitive impairments (Fig.4O and Table 1). We then hypothesized that polymorphisms in TLR4 gene are probably associated with altered spike-induced host immune responses, increasing the risk to develop long-term cognitive deficit in genetically susceptible individuals.

Discussion

Long COVID comprises a myriad of symptoms that emerge after the acute phase of infection, including psychiatric symptoms, and dementia-like cognitive dysfunction (Abdel-Mannan et al., 2020; Almeria et al., 2020; Alonso-Lana et al., 2020; Helms et al., 2020; Woo et al., 2020; Zhou et al., 2021). Clinical studies have largely mapped the spectrum of neurological symptoms in post-COVID patients, but do not provide significant advance in describing the molecular mechanisms that trigger this condition or targets for preventive/therapeutic interventions. In contrast, studies involving COVID-19 preclinical models have entirely focused on the acute impacts of viral infection. Therefore, it is mandatory to develop novel tools to dissect the mechanisms underlying the neurological deficits in long COVID, especially the direct effect of the virus and/or viral products on the brain.

It has been suggested that the S protein can be released from virions(Letarov et al., 2021; Zhang et al., 2020), suggesting that it could directly trigger brain damage. Thus, we speculated that S plays a central role in

bioRxiv preprint doi: https://doi.org/10.1101/2022.06.07.495149; this version posted June 8, 2022. The copyright holder for this preprint (which was not certified by peer review) is the author/funder, who has granted bioRxiv a license to display the preprint in perpetuity. It is made available under aCC-BY-ND 4.0 International license.

neurological dysfunctions associated with COVID-19, independently of SARS-CoV-2 replication in the brain. Previous studies demonstrated that the hippocampus is particularly vulnerable to viral infections(Figueiredo et al., 2019; Jacomy et al., 2006; Vasek et al., 2016). Accordingly, brain scans of COVID-19-recovered patients showed significant changes in hippocampal volume(Lu et al., 2020), an important predictor of cognitive dysfunction in both normal aging and Alzheimer's disease (Peng et al., 2015; Ystad et al., 2009). Here, we developed a rodent model that mimics key neurological features of long COVID through brain icv infusion of S. Using two hippocampal-dependent behavioral paradigms, we found that brain exposure to S disrupts long-term mouse memory, with no early behavioral impact. To our knowledge, this animal model is the first to recapitulate the late cognitive impact of COVID-19.

Synapse damage is a common denominator in a number of memory-related diseases(Bossy-Wetzel et al., 2004), often preceding neurodegeneration. It has been shown that neuroinvasive viruses, such as West Nile virus (WNV), Borna disease virus (BDV) and Zika virus (ZIKV), are also associated with synapse impairment(Figueiredo et al., 2019; Gonzalez-Dunia et al., 2000; Vasek et al., 2016). Likewise, we found that the late cognitive dysfunction induced by S was accompanied by prominent synapse loss in mice hippocampus. Recent data have revealed the upregulation of genes linked to synapse elimination in SARS-CoV-2-infected human brain organoids and in post-mortem samples from COVID-19 patients(Samudyata et al., 2022; Yang et al., 2021). In line, we found that infusion of S into mouse brain induces a late elevation in plasma levels of NFL, an axonal cytoskeleton protein recently identified as a component of pre- and postsynaptic terminals(Yuan et al., 2015). Plasma NFL increase can be

bioRxiv preprint doi: https://doi.org/10.1101/2022.06.07.495149; this version posted June 8, 2022. The copyright holder for this preprint (which was not certified by peer review) is the author/funder, who has granted bioRxiv a license to display the preprint in perpetuity. It is made available under aCC-BY-ND 4.0 International license.

employed as a marker of synapse loss and disease progression in neurodegenerative diseases, including Alzheimer's disease(Bridel et al., 2019). Remarkably, recent data showed that plasma NFL levels are higher in patients with severe COVID-19 compared to healthy age-matched individuals, as well as inversely correlated to the cognitive performance in COVID-19 patients(Kanberg et al., 2020; De Lorenzo et al., 2021), reinforcing the translational potential of our model. Collectively, these findings suggest that brain exposure to S induces the synapse loss and behavioral alterations typical of viral encephalitis, leading to a prolonged neurological dysfunction that can persist long after recovery from the infectious event.

Microglia are the most abundant immune cell type within the CNS and play a critical role in most of the neuroinflammatory diseases (Dheen et al., 2007). In viral encephalitis, microglial cells have both protective and detrimental activities depending on the phase of infection(Chen et al., 2019). Previous studies showed that human coronaviruses can reach the CNS and induce gliosis both in mature and immature brain tissues (Jacomy et al., 2006; Matschke et al., 2020; Vivanti et al., 2020). Here we found that microglial cell lineage BV-2 was impacted by S protein, corroborating recent data showing an increase in proinflammatory mediators in S1-stimulated microglia(Olajide et al., 2022). Since cultured primary cortical neurons were not directly affected by S stimulation, our *in vitro* results indicate that microglia could be seen as the main cell type affected by exposure to SARS-CoV-2 S protein.

It is well known that viral infections are often associated with excessive activation of inflammatory and immune responses, which may in turn elicit and/or accelerate brain neurodegeneration(Zhou et al., 2013). Here, we found that S-

bioRxiv preprint doi: https://doi.org/10.1101/2022.06.07.495149; this version posted June 8, 2022. The copyright holder for this preprint (which was not certified by peer review) is the author/funder, who has granted bioRxiv a license to display the preprint in perpetuity. It is made available under aCC-BY-ND 4.0 International license.

infused mice presented late microglial activation, but not astrocyte reactivity, similar to observed in other animal models of viral encephalitis(Figueiredo et al., 2019; Vasek et al., 2016). Hippocampal increased levels of proinflammatory mediators were found only at late time points after S infusion, showing a temporal correlation with synaptic loss and cognitive dysfunctions. Conversely, we found that the downregulation of *IFNAR2* gene occurred shortly after S injection, similar to what is observed in neuronal cells of post-mortem COVID-19 patients(Yang et al., 2021). This finding corroborates recent evidence demonstrating that SARS-CoV-2 may evade innate immune through modulation of type-I IFN responses (Thorne et al., 2022). In addition to the role of the innate immune response, the potential role of autoimmune mechanisms and the induction of autoantibodies production in long COVID is also under debate(Dotan et al., 2021). We found no circulating antibodies against S protein in our model, suggesting that S-induced cognitive dysfunction is not mediated by antibodies. Altogether, our results show that brain exposure to S induces an early negative modulation of the main receptor involved in type-I IFN response followed by a late proinflammatory process in the hippocampus.

A complement-microglial axis has emerged as one of the key triggers of synapse loss in memory-related diseases(Hong et al., 2016; Stevens et al., 2007). The classical complement cascade, a central player of innate immune pathogen defense, orchestrates synaptic pruning by microglia during physiological and pathological conditions(Schafer et al., 2012; Severance et al., 2014). We have previously reported that hippocampal synapses are phagocytosed by microglia during ZIKV brain infection, in a process dependent on C1q and C3(Figueiredo et al., 2019). Moreover, Vasek and colleagues (2016)

bioRxiv preprint doi: https://doi.org/10.1101/2022.06.07.495149; this version posted June 8, 2022. The copyright holder for this preprint (which was not certified by peer review) is the author/funder, who has granted bioRxiv a license to display the preprint in perpetuity. It is made available under aCC-BY-ND 4.0 International license.

showed hippocampal synapse loss in post-mortem samples of patients with WNV neuroinvasive disease, as well as complement-dependent microglial synapse engulfment in both WNV-infected and -recovered mice(Vasek et al., 2016). Accordingly, we demonstrated that cognitive impairment induced by S protein is associated with hippocampal C1q upregulation and microglial engulfment of presynaptic terminals. Additionally, chronic C1q neutralization preserved memory function in S-infused mice, supporting the role of C1q-mediated synaptic pruning as an important mediator of long COVID cognitive impairment.

The pattern recognition receptor TLR4 has been implicated in the neuropathology of viral encephalitis classically associated with memory impairment, including those caused by WNV, Japanese encephalitis virus (JEV) and BDV, as well as age-related neurodegenerative diseases(Cui et al., 2020; Han et al., 2014; Sabouri et al., 2014; Tang et al., 2021). Notably, *in silico* simulations predicted that the S protein could be recognized by the TLR4(Bhattacharya et al., 2020; Choudhury and Mukherjee, 2020), with this interaction activating the inflammatory signaling, independently of ACE2(Frank et al., 2022; Olajide et al., 2022; Shirato and Kizaki, 2021; Zhao et al., 2021). Accordingly, here we found that a single brain infusion of S protein induced hippocampal TLR4 upregulation. To gain further insight into the role played by TLR4 in COVID-19-induced brain dysfunction, we first performed the pharmacological blockage of TLR4 signal transduction early after S protein brain infusion. This strategy significantly prevented the long-term cognitive impairment observed in our model. Likewise, late cognitive impairment induced by S protein was absent in TLR4-deficient mice, in accordance with previous findings in animal models of dementia(Balducci et al., 2017; Zhong et al., 2020).

bioRxiv preprint doi: https://doi.org/10.1101/2022.06.07.495149; this version posted June 8, 2022. The copyright holder for this preprint (which was not certified by peer review) is the author/funder, who has granted bioRxiv a license to display the preprint in perpetuity. It is made available under aCC-BY-ND 4.0 International license.

Remarkably, we also found that S-induced plasma NFL increase was dependent on TLR4 activation, as early TLR4 inhibition mitigated changes in NFL levels. Together, our findings strongly suggest that brain dysfunction in post-COVID is associated to S-induced TLR4 signaling in microglial cells(Paludan and Mogensen, 2022; Sohn et al., 2020).

The engagement of complement and TLRs in signaling crosstalk has been proposed to regulate immune and inflammatory responses in neurodegenerative diseases(Yang et al., 2020). Indeed, it was shown that TLR4 activation induces the upregulation of complement components in the mouse hippocampus (Hajishengallis and Lambris, 2016; Xin et al., 2019). Given the role of complement activation in synaptic pruning, we hypothesized that TLR4 is the molecular switch that regulates microglial synaptic engulfment. Our data showed that absence of TLR4 confers protection against S-induced synaptic pruning, reinforcing the notion that aberrant immunity activation disrupts synaptic integrity and leads to cognitive dysfunction following pathogenic insult.

Finally, and relevantly, we validated our preclinical findings by examining whether TLR4 genetic variants could be associated with poor cognitive outcome in COVID-19 patients with mild disease. In a cohort of mild COVID-19 patients carrying the GG genotype of *TLR4* -2604G>A (rs10759931) variant, we identified a significant association between this genotype and the risk for cognitive impairment after SARS-CoV-2 infection. The G allele has already been associated with increased risk for different disorders with immunological basis, including cardiovascular diseases(Semlali et al., 2019), diabetes-associated retinopathy(Singh et al., 2014), cancer(Song et al., 2009), and asthma(Kerkhof et al., 2010). On the other hand, the A allele can affect the binding affinity of the

bioRxiv preprint doi: https://doi.org/10.1101/2022.06.07.495149; this version posted June 8, 2022. The copyright holder for this preprint (which was not certified by peer review) is the author/funder, who has granted bioRxiv a license to display the preprint in perpetuity. It is made available under aCC-BY-ND 4.0 International license.

TLR4 promoter to transcription factors, culminating in lower expression of this gene in the allele carriers(Ferronato et al., 2013). Taken together, our findings suggest that the complex crosstalk between TLR4, complement system and neuroinflammation are important events that determines the development of neurological symptoms in long COVID patients.

The impact of long COVID emerges as a major public health concern, due to the high prevalence of prolonged neurological symptoms among survivors. Therefore, strategies designed to prevent or treat neurological long COVID symptoms constitute an unmet clinical need. Our study described a new animal model that recapitulates the long-term impact of the exposure to SARS-CoV-2 S protein on cognitive function. We found that S-induced cognitive impairment triggers innate immunity activation through TLR4, culminating with microgliosis, neuroinflammation and synaptic pruning. The translational value of our model is supported by the correlation between increased plasma NFL and behavioral deficits, as well as by the association between TLR4 genetic status and SARS-CoV-2 cognitive outcomes of recovered COVID-19 patients. Altogether, our findings open new avenues for the establishment of interventional strategies towards prevention and/or treatment of the long-term brain outcomes of COVID-19.

Material and Methods

Animals

Eight to twelve-week-old male Swiss were used in this study. In some experiments, TLR4$^{-/-}$ mice on the C57BL/6 background were used. Animals were housed in groups of five per cage with free access to food and water, under a

bioRxiv preprint doi: https://doi.org/10.1101/2022.06.07.495149; this version posted June 8, 2022. The copyright holder for this preprint (which was not certified by peer review) is the author/funder, who has granted bioRxiv a license to display the preprint in perpetuity. It is made available under aCC-BY-ND 4.0 International license.

12 h light/dark cycle, with controlled temperature and humidity. All procedures followed the “Principles of Laboratory Animal Care” (US National Institutes of Health) and were approved by the Institutional Animal Care and Use Committee of the Federal University of Rio de Janeiro (protocol number 068/2).

Spike intracerebroventricular infusion

The recombinant trimeric SARS-CoV-2 spike protein (S; 1-1208aa) in the prefusion conformation produced in HEK293 cells was obtained from Cell Culture Engineering Laboratory (LECC) of COPPE/UFRJ and was produced as described elsewhere (Cunha et al., 2021). For intracerebroventricular (icv.) infusion of the S protein, mice were anesthetized with 2.5% isoflurane (Cristália; São Paulo, Brazil) using a vaporizer system (Norwell, MA), and a 2.5 mm-long needle was unilaterally inserted 1 mm to the right of the midline point equidistant from each eye and parallel to a line drawn through the anterior base of the eye (REF). Using a Hamilton syringe, 6.5 µg S protein or vehicle (PBS; 137 mM NaCl, 10 mM sodium phosphate, 2.7 mM KCl, pH 7.4) were slowly infused. In order to assess antibody production following S administration, mice received 10 µg S protein or vehicle (PBS) subcutaneously (sc), and boosted after 15 days. The trials were divided into two distinct stages: early phase (assessments performed up to one week after administration) and late phase (between 30 and 45 days after administration).

Pharmacological treatments

For TLR4 blockade, TAK-242 (Millipore) was diluted in sterile saline (vehicle) and injected intraperitoneally (ip; 2mg/kg). Mice received either vehicle or TAK for 7 days beginning immediately after S protein icv. administration. For

bioRxiv preprint doi: https://doi.org/10.1101/2022.06.07.495149; this version posted June 8, 2022. The copyright holder for this preprint (which was not certified by peer review) is the author/funder, who has granted bioRxiv a license to display the preprint in perpetuity. It is made available under aCC-BY-ND 4.0 International license.

brain C1q blockade, mice received icv. injections of vehicle (PBS) or an antibody against C1q (0.3 µg; Abcam #11861) twice a week for 30 days after S brain infusion.

Behavioral tests

Open field test: Animals were placed in the center of an arena (30 × 30 × 45 cm) divided in nine imaginary quadrants, and exploration was assessed for 5 min. The arena was thoroughly cleaned with 70% ethanol in between trials to eliminate olfactory cues. Total locomotor activity and time spent at central or peripheral quadrants were analyzed using ANY-maze software (Stoelting Company).

Novel object recognition (NOR) test: The test was carried out in an arena measuring 30 × 30 × 45 cm. Before training, each animal was submitted to a 5-min habituation session in the empty arena. Test objects were made of plastic and had different shapes, colors, sizes, and textures. Innate object preferences or neophobia were excluded in preliminary tests. Mice explored the configuration of two identical objects during a 5-min acquisition trial. After 90 min, mice were submitted to a 5-min retention trial, during which one of the familiar objects was replaced by an unfamiliar new one. Sniffing and touching the object were considered exploratory behavior. Results were expressed as a percentage of time exploring each object during the training or test sessions, or as total exploration during each session. Data were analyzed using a one-sample Student's *t*-test comparing the mean exploration percentage time for each object with the chance value of 50%. Animals that recognize the familiar object as such (i.e., learn the task) explore the novel object >50% of the total time.

bioRxiv preprint doi: https://doi.org/10.1101/2022.06.07.495149; this version posted June 8, 2022. The copyright holder for this preprint (which was not certified by peer review) is the author/funder, who has granted bioRxiv a license to display the preprint in perpetuity. It is made available under aCC-BY-ND 4.0 International license.

Morris Water Maze (MWM): The apparatus used for the water maze task was a circular tank (1.2 m diameter) filled with water maintained at 20 ± 0.5 °C. The tank was located in a test room containing prominent visual cues. Mice were trained to swim to a 11 cm diameter circular platform submerged 1.5 cm beneath the surface of the water and invisible to the mice while swimming. The platform was located in a fixed position, equidistant from the center and the wall of the tank. Mice were subjected to four training trials per day (inter-trial interval, 10 min). On each trial, mice were placed into the tank at one of four designated start points in a pseudorandom order. Mice were allowed to find and escape onto the submerged platform. If they failed to find the platform within 60 sec, they were manually guided to the platform and allowed to remain for 10 sec. Mice were trained for four consecutive days. The probe trial was assessed 24 hours after the last training session and consisted of a 60 sec free swim in the pool without the platform. Data were collected using the ANY-maze behavioral tracking software (Stoelting).

Rotarod: The test was performed in a mouse rotarod apparatus (Insight Ltda.,Brazil), as previously described (Figueiredo et al., 2019). Briefly, mice were individually placed in the apparatus floor for 3 minutes followed by a 2-min habituation session to the cylinder rod. The test phase consisted of tree trials (inter-trial interval, 60 min) in which animals were placed on the top of the rod rotating at increasing speed (minimal speed 16 rpm, maximal speed 36 rpm with acceleration rate 3.7 rpm). Latency to fall was recorded for a 5 min period, and results are expressed as average latency in the test phase.

bioRxiv preprint doi: https://doi.org/10.1101/2022.06.07.495149; this version posted June 8, 2022. The copyright holder for this preprint (which was not certified by peer review) is the author/funder, who has granted bioRxiv a license to display the preprint in perpetuity. It is made available under aCC-BY-ND 4.0 International license.

Tissue collection

Animals were anesthetized (90 mg/kg ketamine and 4.5 mg/kg xylazine, i.p.) before perfusion with ice-cold PBS at early and late phases of the model. Hippocampal tissues were dissected immediately after perfusion, frozen in liquid nitrogen and stored at -80ºC before RNA extraction. For immunofluorescence studies, perfusion was performed with 4% PFA, and brains were fixed for 24 h before paraffin processing.

Cell culture and treatments

Primary neuronal cortical culture was prepared as previously described (Diniz et al., 2012). Briefly, dissociated cerebral cortices were harvested from embryonic day 14 Swiss mice and cultured in neurobasal medium (Invitrogen) supplemented with B-27, penicillin, streptomycin, l-glutamine, fungizone and cytosine arabinose, and maintained at 37ºC with 5% CO_2. Neurons were seeded at a density of 50.000-150.000 neurons/well on a 13mm diameter poly-D-lysine-coated well (10µg/mL; Sigma). One week after dissociation, neuronal cell cultures were treated with PBS or spike protein (1µg/mL) for 24 h. Later, cells were fixed in 4% PFA, 6% sucrose in PBS for 10 min before immunocytochemistry assay.

The murine BV-2 cell line was cultured in DMEM supplemented with 10% FBS, and 1% streptomycin/penicillin, and seeded at a density of 100.000 cells/well on a 13mm diameter poly-D-lysine-coated well. Next, cells were treated with PBS or spike protein (1µg/mL) for 24 h and fixed as mentioned above.

RNA extraction and qPCR

bioRxiv preprint doi: https://doi.org/10.1101/2022.06.07.495149; this version posted June 8, 2022. The copyright holder for this preprint (which was not certified by peer review) is the author/funder, who has granted bioRxiv a license to display the preprint in perpetuity. It is made available under aCC-BY-ND 4.0 International license.

RNA extraction of hippocampal tissue and cell cultures was performed using Trizol® reagent (Invitrogen), in accordance with manufacturer's instructions. Sample concentration and purity was assessed using a NanoDrop 1000 spectrophotometer. (ThermoScientific). Only preparations with absorbance ratios >1.8 and no signs of RNA degradation were used. One µg of total RNA was reverse transcribed using the High-Capacity cDNA Reverse Transcription Kit (Applied Biosystems), according to the manufacturer's instructions. qPCR was performed using a QuantStudio 5 PCR system (Applied Biosystems) with reactions performed in triplicate. Briefly, qPCRs were run using Power SYBR Green PCR Master Mix (Life Technologies), and 10 ng of template cDNA in a 10 µL reaction volume. The primers used are listed in Supplementary Table 2. Cycle threshold (Ct) values were normalized to a control gene (β-actin) and analyzed using the ΔΔCt method to generate fold change values ($2^{-\Delta\Delta CT}$).

Immunofluorescence assay

Slides containing the hippocampal formation were deparaffinized, and antigen retrieval was carried out by incubation in citrate buffer solution (pH 6.0) at 95ºC for 40 min. Afterwards, permeabilization was performed with 0.025% Triton in PBS, followed by incubation with blocking buffer (PBS containing 0.025% Triton, 3% BSA, and 5% normal goat serum) for 2 h. Next, slides were incubated overnight with primary antibodies against IBA-1 (WAKO; 1:800#019-19741), synaptophysin (Vector Laboratories; 1:200 #S285), Homer-1 (Abcam; 1:100 #184955), or GFAP (Sigma; 1:500 #G3893). For immunocytochemistry, wells were washed three times with PBS, and incubated for 1 h with blocking buffer, followed by overnight incubation with primary antibodies against β3-

bioRxiv preprint doi: https://doi.org/10.1101/2022.06.07.495149; this version posted June 8, 2022. The copyright holder for this preprint (which was not certified by peer review) is the author/funder, who has granted bioRxiv a license to display the preprint in perpetuity. It is made available under aCC-BY-ND 4.0 International license.

tubulin (Promega; 1:1000 #G712A), Iba-1 (1:1000), synaptophysin or Homer-1. For visualization, sections or wells were incubated with AlexaFluor 488- or 546-conjugated secondary antibodies for 2 h at room temperature, washed with PBS and mounted in Fluoroshield with DAPI (Sigma).

The β3-tubulin immunoreactivity in cortical neurons, Iba-1 immunoreactivity in BV-2 cells, as well as microglia density and morphology in Iba-1 immunostained brain sections were photographed using a Slight DS-5-M1 digital camera (Nikon,Melville,NY) connected to an epifluorescence Nikon Eclipse 50i light microscope, under a 20 or 40x objective. Microglia morphology was assessed evaluating the number of branches emanating from their soma (Lopez-Rodrigues et al., 2015). Briefly, type I and type II cells were described as surveillant microglia and present smaller soma and less than 5 thin branches. Type III, IV and V microglia are characterized as reactive microglia, and present more than 4 branches, and thicker branches and bigger soma are observed (Lopez-Rodrigues et al., 2015). Optical density for β3-tubulin and Iba-1 was measured using ImageJ v1.53 and normalized by total DAPI stains. Pyknotic nuclei were analyzed using DAPI stains with 400x magnification and normalized by the total DAPI-stained nuclei observed. In order to determine the synaptic density or synapse engulfment, 9-12 confocal z-stacks (0,35um/z-stack) were obtained using a Leica TSE-SPE3 confocal microscope (Figure 1) or using a Zeiss Cell Observer Spining Disk Confocal microscope (Figure 4) at 630x magnification, and each z-stack was individually analyzed using the ImageJ v1.53 plugin SynQuant automated synapse counter (Wang et al., 2020). Quantitative colocalization of post- (Homer-1) and presynaptic (synaptophysin)

bioRxiv preprint doi: https://doi.org/10.1101/2022.06.07.495149; this version posted June 8, 2022. The copyright holder for this preprint (which was not certified by peer review) is the author/funder, who has granted bioRxiv a license to display the preprint in perpetuity. It is made available under aCC-BY-ND 4.0 International license.

markers, or Iba-1 and synaptophysin in control mice were used to normalize the ratio of preserved synaptic puncta and synaptic engulfment, respectively.

Enzyme-linked immunosorbent assay (ELISA)

The detection of serum anti-spike IgG was carried out as previously described(Fernandes-siqueira et al., 2022). Briefly, 96-well plates (Corning™ Costar™, Life Science) were coated with 50 µl per well of S protein at 4µg/ml in PBS and incubated at 4°C overnight. Plates were washed with PBS-T (0.01% Tween20 in PBS) and incubated with blocking buffer (3% BSA in PBS-T) for 1h. Next, 80 µL serum samples diluted 1:50 in 1% BSA in PBS-T were added to each well. After 2 h at room temperature, plates were washed with PBS-T and 50 µL of the detection antibody conjugated with HRP (Fc-specific anti-mouse IgG, Sigma-Aldrich) at a 1:10,000 dilution were incubated for 1 h. Fifty µL per well of 3,3′,5,5′-Tetramethylbenzidine dihydrochloride (TMB substrate solution, Thermo Fisher) was added, and the reaction was stopped with 3 M hydrochloric acid. Absorbance values at 450 nm were determined on a VICTOR Multilabel plate reader (PerkinElmer).

For cytokine measurements, hippocampus was homogenized in cold RIPA buffer (150 mM NaCl, 1% Triton X-100, 0.5% sodium deoxycholate, 0.1% SDS, 50 mM Tris Base, 2 mM PMSF, pH 8), and supernatant was collected after centrifugation at 14,000 *g* for 10 min at 4°C. Protein concentration as determined using the BCA Protein Assay (Thermo Scientific). Samples diluted 1:10 in RIPA buffer were used for the detection of TNF (BD Biosciences) and IL1β (R&D Systems) by ELISA according to manufacturer's instructions. Results were expressed as pg/µg protein.

bioRxiv preprint doi: https://doi.org/10.1101/2022.06.07.495149; this version posted June 8, 2022. The copyright holder for this preprint (which was not certified by peer review) is the author/funder, who has granted bioRxiv a license to display the preprint in perpetuity. It is made available under aCC-BY-ND 4.0 International license.

Neurofilament light chain (NFL) measurements

Mouse plasma NFL concentration was measured in triplicate using ultra-sensitive single molecule array (Simoa) technique on the Simoa SR-X™ Analyzer, using Simoa NF-Light Advantage according to the manufacturer's instructions (Quanterix). Briefly, plasma samples were thawed at room temperature for one hour and then centrifuged at 10,000 RCF for 5 minutes at 24°C. Samples were diluted 1:4 with sample diluent and applied to the plate in duplicate. Paramagnetic beads coated with capture anti-NFL were incubated with a biotinylated anti-NfL detection antibody, followed by incubation with a streptavidin-β-galactosidase complex. A fluorescent signal proportional to the concentration of NfL was generated after the addition of the substrate resorufin β-D-galactopyranoside. Controls were used to validate the detection limit of 0.0552 pg/mL. All coefficients of variance (CVs) of duplicate measurements were below 20%.

Study population and cognitive assessment

Post-COVID-19 outpatients were evaluated between December 2020 and July 2021 by a multidisciplinary team of neurologists and neuropsychologists at the Gaffrée and Guinle University Hospital (Rio de Janeiro, Brazil). Inclusion criteria included: COVID-19 diagnosis confirmed by PCR or serological diagnosis, fulfilling criteria of mild disease (not require hospitalization and symptoms that not included dyspnea); assessment performed at least 15 days after the end of symptoms, blood collection and neurocognitive evaluation consent. Exclusion criteria included: age under 18 years old; individuals with previously known cognitive impairment or other neuropsychiatrist disorders that

bioRxiv preprint doi: https://doi.org/10.1101/2022.06.07.495149; this version posted June 8, 2022. The copyright holder for this preprint (which was not certified by peer review) is the author/funder, who has granted bioRxiv a license to display the preprint in perpetuity. It is made available under aCC-BY-ND 4.0 International license.

could interfere with the test results. All study subjects had their detailed clinical history recorded and were subjected to complete physical and neurological examination. This work was approved by the Brazilian Ethics Committee (CONEP, CAAE 33659620.1.1001.5258). All participants signed the informed consent term, agreeing to participate in this research.

Neurocognitive status was assessed using the Symbol Digit Modalities Test (SDMT), a screening test developed to identify individuals with cognitive impairment through the domains of attention, processing speed and motor skills(Giménez-Garzó et al., 2021). The raw score of the SDMT is converted to scaled scores (M = 10, SD = 3) using the cumulative frequency distribution of the test in order to normalize test score distributions. The resulting scaled scores is regressed on age, age-squared, sex, and education. After the evaluation, the participants of the study were divided into two main subgroups, “with cognitive deficit” and “without cognitive deficit”.

Sample collection and genotyping

Blood samples were collected and centrifuged at 1.500 *g* at 4 °C for 15 min to separate the buffy coat from plasma. Genomic DNA (gDNA) was extracted using the PureLink Genomic DNA Mini Kit (ThermoFisher Scientific). The quality of the gDNA was determined using NanoDrop 2000 (ThermoFisher Scientific) followed by quantification using the Qubit dsDNA HS Assay Kit (ThermoFisher Scientific) and Qubit Fluorometer 3.0 (Thermo Fisher Scientific).

The *TLR4* -2604G>A (rs10759931) and *TLR4* - 2272A>G (rs2737190) variants were genotyped with allelic discrimination using TaqMan qPCR system (ThermoFisher Scientific). The probes were produced by Applied Biosystems

bioRxiv preprint doi: https://doi.org/10.1101/2022.06.07.495149; this version posted June 8, 2022. The copyright holder for this preprint (which was not certified by peer review) is the author/funder, who has granted bioRxiv a license to display the preprint in perpetuity. It is made available under aCC-BY-ND 4.0 International license.

[rs10759931 (C___2704046_10) and rs2737190 (C___2704047_10)]. Briefly, genotyping was performed in a 20 µL reaction mixture containing 10 ng DNA, TaqMan Universal PCR Master Mix (1X), Probe TaqMan Gene Expression Assay (1X), and DNAse-free water for the final volume. The reaction was carried out in the following conditions: an UNG incubation step of 2 min at 50 °C, polymerase activation for 10 min at 95 °C, followed by 40 cycles of 15 s at 95 °C for denaturation and 60 s at 60 °C for annealing/extension. The amplification and reading of the plates were performed in the QuantStudio 5 Real-Time PCR System (Applied Biosystems).

Illustrations

Illustrations in figures 1A, 3G and 4C and M were created using MindtheGraph (www.mindthegraph.com; under FFD subscription) and subsequently modified (free culture Creative Commons license).

Data analysis

The software Prism v8 (GraphPad) was used for all statistical tests, and values of $p \leq 0.05$ were considered statistically significant. Student's *t*-test was applied to analyze qPCR, ELISA, and immunohistochemical data. For NOR experiments, data were analyzed using a one-sample Student's *t*-test compared to a fixed value of 50%. MWM and NfL measurements were analyzed using repeated measures or one-way ANOVA followed by Tukey's test, respectively. Allelic frequencies were determined by direct count of the alleles. Genotypic distributions in Hardy–Weinberg equilibrium were evaluated by two-tailed χ^2-test. The significant differences in allelic and genotypic frequencies were evaluated by Fisher's exact test and two-tailed χ^2-test.

bioRxiv preprint doi: https://doi.org/10.1101/2022.06.07.495149; this version posted June 8, 2022. The copyright holder for this preprint (which was not certified by peer review) is the author/funder, who has granted bioRxiv a license to display the preprint in perpetuity. It is made available under aCC-BY-ND 4.0 International license.

References

Abdel-Mannan, O., Eyre, M., Löbel, U., Bamford, A., Eltze, C., Hameed, B., Hemingway, C., and Hacohen, Y. (2020). Neurologic and Radiographic Findings Associated With COVID-19 Infection in Children. JAMA Neurol. *77*, 1440–1445. https://doi.org/10.1001/jamaneurol.2020.2687.

Almeria, M., Cejudo, J.C., Sotoca, J., Deus, J., and Krupinski, J. (2020). Cognitive profile following COVID-19 infection: Clinical predictors leading to neuropsychological impairment. Brain, Behav. Immun. - Heal. *9*, 100163. https://doi.org/10.1016/j.bbih.2020.100163.

Alonso-Lana, S., Marquié, M., Ruiz, A., and Boada, M. (2020). Cognitive and Neuropsychiatric Manifestations of COVID-19 and Effects on Elderly Individuals With Dementia. Front. Aging Neurosci. *12*, 588872. https://doi.org/10.3389/fnagi.2020.588872.

Balducci, C., Frasca, A., Zotti, M., La Vitola, P., Mhillaj, E., Grigoli, E., Iacobellis, M., Grandi, F., Messa, M., Colombo, L., et al. (2017). Toll-like receptor 4-dependent glial cell activation mediates the impairment in memory establishment induced by β-amyloid oligomers in an acute mouse model of Alzheimer's disease. Brain. Behav. Immun. *60*, 188–197. https://doi.org/10.1016/j.bbi.2016.10.012.

Bhattacharya, M., Sharma, A.R., Mallick, B., Sharma, G., Lee, S.-S., and Chakraborty, C. (2020). Immunoinformatics approach to understand molecular interaction between multi-epitopic regions of SARS-CoV-2 spike-protein with TLR4/MD-2 complex. Infect. Genet. Evol. J. Mol. Epidemiol. Evol. Genet. Infect. Dis. *85*, 104587. https://doi.org/10.1016/j.meegid.2020.104587.

Blomberg, B., Mohn, K.G.-I., Brokstad, K.A., Zhou, F., Linchausen, D.W., Hansen, B.-A., Lartey, S., Onyango, T.B., Kuwelker, K., Sævik, M., et al. (2021). Long COVID in a prospective cohort of home-isolated patients. Nat. Med. *27*, 1607–1613. https://doi.org/10.1038/s41591-021-01433-3.

Bossy-Wetzel, E., Schwarzenbacher, R., and Lipton, S.A. (2004). Molecular pathways

bioRxiv preprint doi: https://doi.org/10.1101/2022.06.07.495149; this version posted June 8, 2022. The copyright holder for this preprint (which was not certified by peer review) is the author/funder, who has granted bioRxiv a license to display the preprint in perpetuity. It is made available under aCC-BY-ND 4.0 International license.

to neurodegeneration. Nat. Med. *10 Suppl*, S2-9. https://doi.org/10.1038/nm1067.

Bridel, C., van Wieringen, W.N., Zetterberg, H., Tijms, B.M., Teunissen, C.E., Alvarez-Cermeño, J.C., Andreasson, U., Axelsson, M., Bäckström, D.C., Bartos, A., et al. (2019). Diagnostic Value of Cerebrospinal Fluid Neurofilament Light Protein in Neurology: A Systematic Review and Meta-analysis. JAMA Neurol. *76*, 1035–1048. https://doi.org/10.1001/jamaneurol.2019.1534.

Buzhdygan, T.P., DeOre, B.J., Baldwin-Leclair, A., Bullock, T.A., McGary, H.M., Khan, J.A., Razmpour, R., Hale, J.F., Galie, P.A., Potula, R., et al. (2020). The SARS-CoV-2 spike protein alters barrier function in 2D static and 3D microfluidic in-vitro models of the human blood-brain barrier. Neurobiol. Dis. *146*, 105131. https://doi.org/10.1016/j.nbd.2020.105131.

Chen, Z., Zhong, D., and Li, G. (2019). The role of microglia in viral encephalitis: a review. J. Neuroinflammation *16*, 76. https://doi.org/10.1186/s12974-019-1443-2.

Choudhury, A., and Mukherjee, S. (2020). In silico studies on the comparative characterization of the interactions of SARS-CoV-2 spike glycoprotein with ACE-2 receptor homologs and human TLRs. J. Med. Virol. *92*, 2105–2113. https://doi.org/10.1002/jmv.25987.

Cui, W., Sun, C., Ma, Y., Wang, S., Wang, X., and Zhang, Y. (2020). Inhibition of TLR4 Induces M2 Microglial Polarization and Provides Neuroprotection via the NLRP3 Inflammasome in Alzheimer's Disease. Front. Neurosci. *14*, 444. https://doi.org/10.3389/fnins.2020.00444.

Cunha, L.E.R., Stolet, A.A., Strauch, M.A., Pereira, V.A.R., Dumard, C.H., Gomes, A.M.O., Monteiro, F.L., Higa, L.M., Souza, P.N.C., Fonseca, J.G., et al. (2021). Polyclonal F(ab')(2) fragments of equine antibodies raised against the spike protein neutralize SARS-CoV-2 variants with high potency. IScience *24*, 103315. https://doi.org/10.1016/j.isci.2021.103315.

Dheen, S.T., Kaur, C., and Ling, E.-A. (2007). Microglial activation and its implications in the brain diseases. Curr. Med. Chem. *14*, 1189–1197.

bioRxiv preprint doi: https://doi.org/10.1101/2022.06.07.495149; this version posted June 8, 2022. The copyright holder for this preprint (which was not certified by peer review) is the author/funder, who has granted bioRxiv a license to display the preprint in perpetuity. It is made available under aCC-BY-ND 4.0 International license.

https://doi.org/10.2174/092986707780597961.

Diniz, L.P., Almeida, J.C., Tortelli, V., Vargas Lopes, C., Setti-Perdigão, P., Stipursky, J., Kahn, S.A., Romão, L.F., de Miranda, J., Alves-Leon, S.V., et al. (2012). Astrocyte-induced synaptogenesis is mediated by transforming growth factor β signaling through modulation of D-serine levels in cerebral cortex neurons. J. Biol. Chem. *287*, 41432–41445. https://doi.org/10.1074/jbc.M112.380824.

Dotan, A., Muller, S., Kanduc, D., David, P., Halpert, G., and Shoenfeld, Y. (2021). The SARS-CoV-2 as an instrumental trigger of autoimmunity. Autoimmun. Rev. *20*, 102792. https://doi.org/10.1016/j.autrev.2021.102792.

Edén, A., Kanberg, N., Gostner, J., Fuchs, D., Hagberg, L., Andersson, L.-M., Lindh, M., Price, R.W., Zetterberg, H., and Gisslén, M. (2021). CSF Biomarkers in Patients With COVID-19 and Neurologic Symptoms: A Case Series. Neurology *96*, e294–e300. https://doi.org/10.1212/WNL.0000000000010977.

Farhadian, S., Glick, L.R., Vogels, C.B.F., Thomas, J., Chiarella, J., Casanovas-Massana, A., Zhou, J., Odio, C., Vijayakumar, P., Geng, B., et al. (2020). Acute encephalopathy with elevated CSF inflammatory markers as the initial presentation of COVID-19. BMC Neurol. *20*, 248. https://doi.org/10.1186/s12883-020-01812-2.

Fernandes-siqueira, L., Almeida, F., Ferreira, G., and Salmon, D. (2022). On the caveats of a multiplex test for SARS-CoV-2 to detect seroconversion after infection or vaccination Results. Res. Sq. Prepr. 1–17. .

Ferronato, S., Gomez-Lira, M., Menegazzi, M., Diani, E., Olivato, S., Sartori, M., Scuro, A., Malerba, G., Pignatti, P.F., Romanelli, M.G., et al. (2013). Polymorphism -2604G>A variants in TLR4 promoter are associated with different gene expression level in peripheral blood of atherosclerotic patients. J. Hum. Genet. *58*, 812–814. https://doi.org/10.1038/jhg.2013.98.

Figueiredo, C.P., Barros-Aragão, F.G.Q., Neris, R.L.S., Frost, P.S., Soares, C., Souza, I.N.O., Zeidler, J.D., Zamberlan, D.C., de Sousa, V.L., Souza, A.S., et al. (2019). Zika virus replicates in adult human brain tissue and impairs synapses and memory in mice.

bioRxiv preprint doi: https://doi.org/10.1101/2022.06.07.495149; this version posted June 8, 2022. The copyright holder for this preprint (which was not certified by peer review) is the author/funder, who has granted bioRxiv a license to display the preprint in perpetuity. It is made available under aCC-BY-ND 4.0 International license.

Nat. Commun. *10*. https://doi.org/10.1038/s41467-019-11866-7.

Frank, M.G., Nguyen, K.H., Ball, J.B., Hopkins, S., Kelley, T., Baratta, M. V, Fleshner, M., and Maier, S.F. (2022). SARS-CoV-2 spike S1 subunit induces neuroinflammatory, microglial and behavioral sickness responses: Evidence of PAMP-like properties. Brain. Behav. Immun. *100*, 267–277. https://doi.org/10.1016/j.bbi.2021.12.007.

Giménez-Garzó, C., Fiorillo, A., Ballester-Ferré, M.-P., Gallego, J.-J., Casanova-Ferrer, F., Urios, A., Benlloch, S., Martí-Aguado, D., San-Miguel, T., Tosca, J., et al. (2021). A New Score Unveils a High Prevalence of Mild Cognitive Impairment in Patients with Nonalcoholic Fatty Liver Disease. J. Clin. Med. *10*. https://doi.org/10.3390/jcm10132806.

Gonzalez-Dunia, D., Watanabe, M., Syan, S., Mallory, M., Masliah, E., and De La Torre, J.C. (2000). Synaptic pathology in Borna disease virus persistent infection. J. Virol. *74*, 3441–3448. https://doi.org/10.1128/jvi.74.8.3441-3448.2000.

Hajishengallis, G., and Lambris, J.D. (2016). More than complementing Tolls: complement-Toll-like receptor synergy and crosstalk in innate immunity and inflammation. Immunol. Rev. *274*, 233–244. https://doi.org/10.1111/imr.12467.

Han, Y.W., Choi, J.Y., Uyangaa, E., Kim, S.B., Kim, J.H., Kim, B.S., Kim, K., and Eo, S.K. (2014). Distinct dictation of Japanese encephalitis virus-induced neuroinflammation and lethality via triggering TLR3 and TLR4 signal pathways. PLoS Pathog. *10*, e1004319. https://doi.org/10.1371/journal.ppat.1004319.

Helms, J., Kremer, S., Merdji, H., Clere-Jehl, R., Schenck, M., Kummerlen, C., Collange, O., Boulay, C., Fafi-Kremer, S., Ohana, M., et al. (2020). Neurologic Features in Severe SARS-CoV-2 Infection. N. Engl. J. Med. *382*, 2268–2270. https://doi.org/10.1056/NEJMc2008597.

Hong, S., Beja-Glasser, V.F., Nfonoyim, B.M., Frouin, A., Li, S., Ramakrishnan, S., Merry, K.M., Shi, Q., Rosenthal, A., Barres, B.A., et al. (2016). Complement and microglia mediate early synapse loss in Alzheimer mouse models. Science *352*, 712–716. https://doi.org/10.1126/science.aad8373.

bioRxiv preprint doi: https://doi.org/10.1101/2022.06.07.495149; this version posted June 8, 2022. The copyright holder for this preprint (which was not certified by peer review) is the author/funder, who has granted bioRxiv a license to display the preprint in perpetuity. It is made available under aCC-BY-ND 4.0 International license.

Jacomy, H., Fragoso, G., Almazan, G., Mushynski, W.E., and Talbot, P.J. (2006). Human coronavirus OC43 infection induces chronic encephalitis leading to disabilities in BALB/C mice. Virology *349*, 335–346. https://doi.org/10.1016/j.virol.2006.01.049.

Kanberg, N., Ashton, N.J., Andersson, L.-M., Yilmaz, A., Lindh, M., Nilsson, S., Price, R.W., Blennow, K., Zetterberg, H., and Gisslén, M. (2020). Neurochemical evidence of astrocytic and neuronal injury commonly found in COVID-19. Neurology *95*, e1754–e1759. https://doi.org/10.1212/WNL.0000000000010111.

Kerkhof, M., Postma, D.S., Brunekreef, B., Reijmerink, N.E., Wijga, A.H., de Jongste, J.C., Gehring, U., and Koppelman, G.H. (2010). Toll-like receptor 2 and 4 genes influence susceptibility to adverse effects of traffic-related air pollution on childhood asthma. Thorax *65*, 690–697. https://doi.org/10.1136/thx.2009.119636.

Letarov, A. V, Babenko, V. V, and Kulikov, E.E. (2021). Free SARS-CoV-2 Spike Protein S1 Particles May Play a Role in the Pathogenesis of COVID-19 Infection. Biochemistry. (Mosc). *86*, 257–261. https://doi.org/10.1134/S0006297921030032.

De Lorenzo, R., Loré, N.I., Finardi, A., Mandelli, A., Cirillo, D.M., Tresoldi, C., Benedetti, F., Ciceri, F., Rovere-Querini, P., Comi, G., et al. (2021). Blood neurofilament light chain and total tau levels at admission predict death in COVID-19 patients. J. Neurol. *268*, 4436–4442. https://doi.org/10.1007/s00415-021-10595-6.

Lu, Y., Li, X., Geng, D., Mei, N., Wu, P.-Y., Huang, C.-C., Jia, T., Zhao, Y., Wang, D., Xiao, A., et al. (2020). Cerebral Micro-Structural Changes in COVID-19 Patients - An MRI-based 3-month Follow-up Study. EClinicalMedicine *25*, 100484. https://doi.org/10.1016/j.eclinm.2020.100484.

Martin, M. da G.M., Paes, V.R., Cardoso, E.F., Neto, C.E.B.P., Kanamura, C.T., Leite, C. da C., Otaduy, M.C.G., Monteiro, R.A. de A., Mauad, T., da Silva, L.F.F., et al. (2022). Postmortem brain 7T MRI with minimally invasive pathological correlation in deceased COVID-19 subjects. Insights Imaging *13*, 7. https://doi.org/10.1186/s13244-021-01144-w.

Matschke, J., Lütgehetmann, M., Hagel, C., Sperhake, J.P., Schröder, A.S., Edler, C.,

bioRxiv preprint doi: https://doi.org/10.1101/2022.06.07.495149; this version posted June 8, 2022. The copyright holder for this preprint (which was not certified by peer review) is the author/funder, who has granted bioRxiv a license to display the preprint in perpetuity. It is made available under aCC-BY-ND 4.0 International license.

Mushumba, H., Fitzek, A., Allweiss, L., Dandri, M., et al. (2020). Neuropathology of patients with COVID-19 in Germany: a post-mortem case series. Lancet. Neurol. *19*, 919–929. https://doi.org/10.1016/S1474-4422(20)30308-2.

Miron, J., Picard, C., Lafaille-Magnan, M.-É., Savard, M., Labonté, A., Breitner, J., Rosa-Neto, P., Auld, D., and Poirier, J. (2019). Association of TLR4 with Alzheimer's disease risk and presymptomatic biomarkers of inflammation. Alzheimers. Dement. *15*, 951–960. https://doi.org/10.1016/j.jalz.2019.03.012.

Olajide, O.A., Iwuanyanwu, V.U., Adegbola, O.D., and Al-Hindawi, A.A. (2022). SARS-CoV-2 Spike Glycoprotein S1 Induces Neuroinflammation in BV-2 Microglia. Mol. Neurobiol. *59*, 445–458. https://doi.org/10.1007/s12035-021-02593-6.

Paludan, S.R., and Mogensen, T.H. (2022). Innate immunological pathways in COVID-19 pathogenesis. Sci. Immunol. *7*, eabm5505. https://doi.org/10.1126/sciimmunol.abm5505.

Peng, G.-P., Feng, Z., He, F.-P., Chen, Z.-Q., Liu, X.-Y., Liu, P., and Luo, B.-Y. (2015). Correlation of hippocampal volume and cognitive performances in patients with either mild cognitive impairment or Alzheimer's disease. CNS Neurosci. Ther. *21*, 15–22. https://doi.org/10.1111/cns.12317.

Pilotto, A., Masciocchi, S., Volonghi, I., De Giuli, V., Caprioli, F., Mariotto, S., Ferrari, S., Bozzetti, S., Imarisio, A., Risi, B., et al. (2021). Severe Acute Respiratory Syndrome Coronavirus 2 (SARS-CoV-2) Encephalitis Is a Cytokine Release Syndrome: Evidences From Cerebrospinal Fluid Analyses. Clin. Infect. Dis. an Off. Publ. Infect. Dis. Soc. Am. *73*, e3019–e3026. https://doi.org/10.1093/cid/ciaa1933.

Rhea, E.M., Logsdon, A.F., Hansen, K.M., Williams, L.M., Reed, M.J., Baumann, K.K., Holden, S.J., Raber, J., Banks, W.A., and Erickson, M.A. (2020). The S1 protein of SARS-CoV-2 crosses the blood–brain barrier in mice. Nat. Neurosci. https://doi.org/10.1038/s41593-020-00771-8.

Sabouri, A.H., Marcondes, M.C.G., Flynn, C., Berger, M., Xiao, N., Fox, H.S., and Sarvetnick, N.E. (2014). TLR signaling controls lethal encephalitis in WNV-infected

bioRxiv preprint doi: https://doi.org/10.1101/2022.06.07.495149; this version posted June 8, 2022. The copyright holder for this preprint (which was not certified by peer review) is the author/funder, who has granted bioRxiv a license to display the preprint in perpetuity. It is made available under aCC-BY-ND 4.0 International license.

brain. Brain Res. *1574*, 84–95. https://doi.org/10.1016/j.brainres.2014.05.049.

Samudyata, Oliveira, A.O., Malwade, S., de Sousa, N.R., Goparaju, S.K., Lekander, J.G., Orhan, F., Steponaviciute, L., Schalling, M., Sheridan, S.D., et al. (2022). SARS-CoV-2 promotes microglial synapse elimination in human brain organoids. BioRxiv 2021.07.07.451463. https://doi.org/10.1101/2021.07.07.451463.

Schafer, D.P., Lehrman, E.K., Kautzman, A.G., Koyama, R., Mardinly, A.R., Yamasaki, R., Ransohoff, R.M., Greenberg, M.E., Barres, B.A., and Stevens, B. (2012). Microglia sculpt postnatal neural circuits in an activity and complement-dependent manner. Neuron *74*, 691–705. https://doi.org/10.1016/j.neuron.2012.03.026.

Semlali, A., Al Mutairi, M., Oqla Alanazi, I., Awad Aljohi, H., Reddy Parine, N., Alhadheq, A., Al-Jafari, A.A., Mobeirek, A.F., Al Amri, A., Shaik, J.P., et al. (2019). Toll-like receptor 4 polymorphisms in Saudi population with cardiovascular diseases. Mol. Genet. Genomic Med. *7*, e852. https://doi.org/10.1002/mgg3.852.

Severance, E.G., Gressitt, K.L., Buka, S.L., Cannon, T.D., and Yolken, R.H. (2014). Maternal complement C1q and increased odds for psychosis in adult offspring. Schizophr. Res. *159*, 14–19. https://doi.org/10.1016/j.schres.2014.07.053.

Shirato, K., and Kizaki, T. (2021). SARS-CoV-2 spike protein S1 subunit induces pro-inflammatory responses via toll-like receptor 4 signaling in murine and human macrophages. Heliyon *7*, e06187–e06187. https://doi.org/10.1016/j.heliyon.2021.e06187.

Shives, K.D., Tyler, K.L., and Beckham, J.D. (2017). Molecular mechanisms of neuroinflammation and injury during acute viral encephalitis. J. Neuroimmunol. *308*, 102–111. https://doi.org/10.1016/j.jneuroim.2017.03.006.

Singh, K., Kant, S., Singh, V.K., Agrawal, N.K., Gupta, S.K., and Singh, K. (2014). Toll-like receptor 4 polymorphisms and their haplotypes modulate the risk of developing diabetic retinopathy in type 2 diabetes patients. Mol. Vis. *20*, 704–713. .

Sohn, K.M., Lee, S.G., Kim, H.J., Cheon, S., Jeong, H., Lee, J., Kim, I.S., Silwal, P., Kim, Y.J., Paik, S., et al. (2020). COVID-19 Patients Upregulate Toll-like Receptor 4-

bioRxiv preprint doi: https://doi.org/10.1101/2022.06.07.495149; this version posted June 8, 2022. The copyright holder for this preprint (which was not certified by peer review) is the author/funder, who has granted bioRxiv a license to display the preprint in perpetuity. It is made available under aCC-BY-ND 4.0 International license.

mediated Inflammatory Signaling That Mimics Bacterial Sepsis. J. Korean Med. Sci. *35*, e343. https://doi.org/10.3346/jkms.2020.35.e343.

Song, J., Kim, D.Y., Kim, C.S., Kim, H.J., Lee, D.H., Lee, H.M., Ko, W., and Lee, G. (2009). The association between Toll-like receptor 4 (TLR4) polymorphisms and the risk of prostate cancer in Korean men. Cancer Genet. Cytogenet. *190*, 88–92. https://doi.org/10.1016/j.cancergencyto.2008.12.011.

Stevens, B., Allen, N.J., Vazquez, L.E., Howell, G.R., Christopherson, K.S., Nouri, N., Micheva, K.D., Mehalow, A.K., Huberman, A.D., Stafford, B., et al. (2007). The classical complement cascade mediates CNS synapse elimination. Cell *131*, 1164–1178. https://doi.org/10.1016/j.cell.2007.10.036.

Sun, B., Tang, N., Peluso, M.J., Iyer, N.S., Torres, L., Donatelli, J.L., Munter, S.E., Nixon, C.C., Rutishauser, R.L., Rodriguez-Barraquer, I., et al. (2021). Characterization and Biomarker Analyses of Post-COVID-19 Complications and Neurological Manifestations. Cells *10*. https://doi.org/10.3390/cells10020386.

Tang, T., Guo, Y., Xu, X., Zhao, L., Shen, X., Sun, L., and Xie, P. (2021). BoDV-1 infection induces neuroinflammation by activating the TLR4/MyD88/IRF5 signaling pathway, leading to learning and memory impairment in rats. J. Med. Virol. *93*, 6163–6171. https://doi.org/10.1002/jmv.27212.

Thorne, L.G., Bouhaddou, M., Reuschl, A.-K., Zuliani-Alvarez, L., Polacco, B., Pelin, A., Batra, J., Whelan, M.V.X., Hosmillo, M., Fossati, A., et al. (2022). Evolution of enhanced innate immune evasion by SARS-CoV-2. Nature *602*, 487–495. https://doi.org/10.1038/s41586-021-04352-y.

Vasek, M.J., Garber, C., Dorsey, D., Durrant, D.M., Bollman, B., Soung, A., Yu, J., Perez-Torres, C., Frouin, A., Wilton, D.K., et al. (2016). A complement-microglial axis drives synapse loss during virus-induced memory impairment. Nature *534*, 538–543. https://doi.org/10.1038/nature18283.

Vivanti, A.J., Vauloup-Fellous, C., Prevot, S., Zupan, V., Suffee, C., Do Cao, J., Benachi, A., and De Luca, D. (2020). Transplacental transmission of SARS-CoV-2

bioRxiv preprint doi: https://doi.org/10.1101/2022.06.07.495149; this version posted June 8, 2022. The copyright holder for this preprint (which was not certified by peer review) is the author/funder, who has granted bioRxiv a license to display the preprint in perpetuity. It is made available under aCC-BY-ND 4.0 International license.

infection. Nat. Commun. *11*, 3572. https://doi.org/10.1038/s41467-020-17436-6.

Vorhees, C. V, and Williams, M.T. (2006). Morris water maze: procedures for assessing spatial and related forms of learning and memory. Nat. Protoc. *1*, 848–858. https://doi.org/10.1038/nprot.2006.116.

Walls, A.C., Park, Y.-J., Tortorici, M.A., Wall, A., McGuire, A.T., and Veesler, D. (2020). Structure, Function, and Antigenicity of the SARS-CoV-2 Spike Glycoprotein. Cell *181*, 281-292.e6. https://doi.org/https://doi.org/10.1016/j.cell.2020.02.058.

Wang, Q., Nair, M.S., Anang, S., Zhang, S., Nguyen, H., Huang, Y., Liu, L., Ho, D.D., and Sodroski, J.G. (2021). Functional differences among the spike glycoproteins of multiple emerging severe acute respiratory syndrome coronavirus 2 variants of concern. IScience *24*, 103393. https://doi.org/10.1016/j.isci.2021.103393.

Woo, M.S., Malsy, J., Pöttgen, J., Seddiq Zai, S., Ufer, F., Hadjilaou, A., Schmiedel, S., Addo, M.M., Gerloff, C., Heesen, C., et al. (2020). Frequent neurocognitive deficits after recovery from mild COVID-19. Brain Commun. *2*, fcaa205. https://doi.org/10.1093/braincomms/fcaa205.

Xin, Y.-R., Jiang, J.-X., Hu, Y., Pan, J.-P., Mi, X.-N., Gao, Q., Xiao, F., Zhang, W., and Luo, H.-M. (2019). The Immune System Drives Synapse Loss During Lipopolysaccharide-Induced Learning and Memory Impairment in Mice. Front. Aging Neurosci. *11*, 279. https://doi.org/10.3389/fnagi.2019.00279.

Yang, A.C., Kern, F., Losada, P.M., Agam, M.R., Maat, C.A., Schmartz, G.P., Fehlmann, T., Stein, J.A., Schaum, N., Lee, D.P., et al. (2021). Dysregulation of brain and choroid plexus cell types in severe COVID-19. Nature *595*, 565–571. https://doi.org/10.1038/s41586-021-03710-0.

Yang, J., Wise, L., and Fukuchi, K.-I. (2020). TLR4 Cross-Talk With NLRP3 Inflammasome and Complement Signaling Pathways in Alzheimer's Disease. Front. Immunol. *11*, 724. https://doi.org/10.3389/fimmu.2020.00724.

Ystad, M.A., Lundervold, A.J., Wehling, E., Espeseth, T., Rootwelt, H., Westlye, L.T., Andersson, M., Adolfsdottir, S., Geitung, J.T., Fjell, A.M., et al. (2009). Hippocampal

bioRxiv preprint doi: https://doi.org/10.1101/2022.06.07.495149; this version posted June 8, 2022. The copyright holder for this preprint (which was not certified by peer review) is the author/funder, who has granted bioRxiv a license to display the preprint in perpetuity. It is made available under aCC-BY-ND 4.0 International license.

volumes are important predictors for memory function in elderly women. BMC Med. Imaging *9*, 17. https://doi.org/10.1186/1471-2342-9-17.

Yu, J.-T., Miao, D., Cui, W.-Z., Ou, J.-R., Tian, Y., Wu, Z.-C., Zhang, W., and Tan, L. (2012). Common variants in toll-like receptor 4 confer susceptibility to Alzheimer's disease in a Han Chinese population. Curr. Alzheimer Res. *9*, 458–466. https://doi.org/10.2174/156720512800492495.

Yuan, A., Sershen, H., Veeranna, Basavarajappa, B.S., Kumar, A., Hashim, A., Berg, M., Lee, J.-H., Sato, Y., Rao, M. V, et al. (2015). Neurofilament subunits are integral components of synapses and modulate neurotransmission and behavior in vivo. Mol. Psychiatry *20*, 986–994. https://doi.org/10.1038/mp.2015.45.

Zhang, L., Jackson, C.B., Mou, H., Ojha, A., Peng, H., Quinlan, B.D., Rangarajan, E.S., Pan, A., Vanderheiden, A., Suthar, M.S., et al. (2020). SARS-CoV-2 spike-protein D614G mutation increases virion spike density and infectivity. Nat. Commun. *11*, 6013. https://doi.org/10.1038/s41467-020-19808-4.

Zhao, Y., Kuang, M., Li, J., Zhu, L., Jia, Z., Guo, X., Hu, Y., Kong, J., Yin, H., Wang, X., et al. (2021). SARS-CoV-2 spike protein interacts with and activates TLR41. Cell Res. 1–3. https://doi.org/10.1038/s41422-021-00495-9.

Zhong, Q., Zou, Y., Liu, H., Chen, T., Zheng, F., Huang, Y., Chen, C., and Zhang, Z. (2020). Toll-like receptor 4 deficiency ameliorates β2-microglobulin induced age-related cognition decline due to neuroinflammation in mice. Mol. Brain *13*, 20. https://doi.org/10.1186/s13041-020-0559-8.

Zhou, L., Miranda-Saksena, M., and Saksena, N.K. (2013). Viruses and neurodegeneration.

Zhou, Y., Xu, J., Hou, Y., Leverenz, J.B., Kallianpur, A., Mehra, R., Liu, Y., Yu, H., Pieper, A.A., Jehi, L., et al. (2021). Network medicine links SARS-CoV-2/COVID-19 infection to brain microvascular injury and neuroinflammation in dementia-like cognitive impairment. Alzheimers. Res. Ther. *13*, 110. https://doi.org/10.1186/s13195-021-00850-3.

bioRxiv preprint doi: https://doi.org/10.1101/2022.06.07.495149; this version posted June 8, 2022. The copyright holder for this preprint (which was not certified by peer review) is the author/funder, who has granted bioRxiv a license to display the preprint in perpetuity. It is made available under aCC-BY-ND 4.0 International license.

Acknowledgements

The authors thank Luis F. Fragoso and Ana Claudia Rangel for their technical support; Prof. Leda R. Castilho and her team at Cell Culture Engineering Laboratory (LECC) of COPPE/UFRJ for providing the trimeric spike protein in the prefusion conformation; and Prof. João B. Calixto (Centro de Inovação e Ensaios Pré-clínicos- CIENP), Prof. João B. Teixeira da Rocha (Federal University of Santa Maria) and Prof. Andreza F. De Bem (Brazilian Federal University) for thoughtful discussion and manuscript critical reading. This work was was supported by Fundação de Amparo à Pesquisa do Estado do Rio de Janeiro - FAPERJ (F.L.F.D., G.G.F., L.S.A., L.C.C., S.B.A., L.E.B.S., J.L.S., R.C., J.R.C., A.T.P, S.V.A.L, G.F.P., C.P.F.), Instituto Nacional de Ciência e Tecnologia (INCT) Inovação em Medicamentos e Identificação de Novos Alvos Terapêuticos - INCT-INOVAMED (R.C., G.F.P., C.P.F.), INCT de Biologia Estrutural e Bioimagem - INBEB (J.L.S, A.T.P.). Conselho Nacional de Desenvolvimento Científico e Tecnológico - CNPq (G.G.F., H.M.A., L.E.B.S., J.L.S., J.R.C., R.C., A.T.P, S.V.A.L., G.F.P., C.P.F.), Coordenação de Aperfeiçoamento de Pessoal de Nível Superior-CAPES (E.V.L., T.N.S.), and Programa de Pesquisa Para o SUS (PPSUS)/Brazilian Ministry of Health (F.L.F.D., R.C., J.R.C, S.V.A.L., G.F.P., C.P.F).

Contributions

bioRxiv preprint doi: https://doi.org/10.1101/2022.06.07.495149; this version posted June 8, 2022. The copyright holder for this preprint (which was not certified by peer review) is the author/funder, who has granted bioRxiv a license to display the preprint in perpetuity. It is made available under aCC-BY-ND 4.0 International license.

C.P.F., G.F.P., S.V.A.L., A.T.P., J.R.C., R.C., and F.L.F.D. conceived the study. C.P.F., G.F.P., S.V.A.L., A.T.P., F.L.F.D., J.R.C., R.C., J.L.S., and L.E.B.S., contributed to experimental design. F.L.F.D., G.G.F., E.V.L., L.S.A., H.P.M.A., L.C.C., S.M.B.A., and T.N.S. performed experiments in mice and analyzed the data. Molecular experiments and ELISA were performed and analyzed by F.L.F.D., L.C.C., S.M.B.A., and A.T.P. Histological and immunohisto/cytochemistry analyses were performed by G.G.F., C.P.F., and E.V.L. L.E.B.S, L.R., and G.G.F. performed experiments in cell culture. L.A.D. and A.L.S. performed Simoa experiments. E.G.G., M.B.H., K.L.P., C.C.F.V., and S.V.A.L. recruited patients, collected clinical information and performed neuropsychological evaluations. L.A.A.L. performed molecular and serological diagnosis of COVID-19. F.L.F.D. and E.G.G. carried out genotype analyses. F.L.F.D., G.G.F., E.G.G., C.P.F., G.F.P., S.V.A.L., A.T.P., J.R.C., R.C., and L.E.B.S. contributed to critical analysis of the data. F.L.F.D., C.P.F, and G.F.P. wrote the manuscript. All authors read and approved the final version.

bioRxiv preprint doi: https://doi.org/10.1101/2022.06.07.495149; this version posted June 8, 2022. The copyright holder for this preprint (which was not certified by peer review) is the author/funder, who has granted bioRxiv a license to display the preprint in perpetuity. It is made available under aCC-BY-ND 4.0 International license.

Tables

Table 1. *TLR4* rs10759931 and rs2737190 genotype distribution in patients with or without cognitive deficit following COVID-19.

***TLR4* -2604G>A (rs10759931)**	**N (86)**	**Cognitive Deficit (%)**	**No Cognitive Deficit (%)**	***P-value***	**OR (95% CI)**
GG	40	22(55)	18(39)	0.0234*	1.91 (1.083 to 3.301)
GA	35	13(32)	22(48)	0.0209*	0.50 (0.287 to 0.920)
AA	11	5(13)	6(13)	>0,9999	1.00 (0.435 to 2.294)
MAF (A)	0.33				
***TLR4* -2272 A>G (rs2737190)**	**N (83)**	**Cognitive Deficit (%)**	**No Cognitive Deficit (%)**	**P-value**	**OR (95% CI)**
AA	30	14(37)	16(36)	0.8832	1.04 (0.594 to 1.836)
AG	35	16(42)	19(42)	>0,9999	1.0 (0.561 to 1.781)
GG	18	8(21)	10(22)	0.8633	0.94 (0.483 to 1.823)
MAF (G)	0.43				

MAF= minor allele frequency; OR = odds ratio; CI = confidence interval. Data analyzed by χ2-test (two-tailed). *Statistical significance (P<0.05). The reference group in each of the analyses was the most prevalent genotype.

bioRxiv preprint doi: https://doi.org/10.1101/2022.06.07.495149; this version posted June 8, 2022. The copyright holder for this preprint (which was not certified by peer review) is the author/funder, who has granted bioRxiv a license to display the preprint in perpetuity. It is made available under aCC-BY-ND 4.0 International license.

Figures

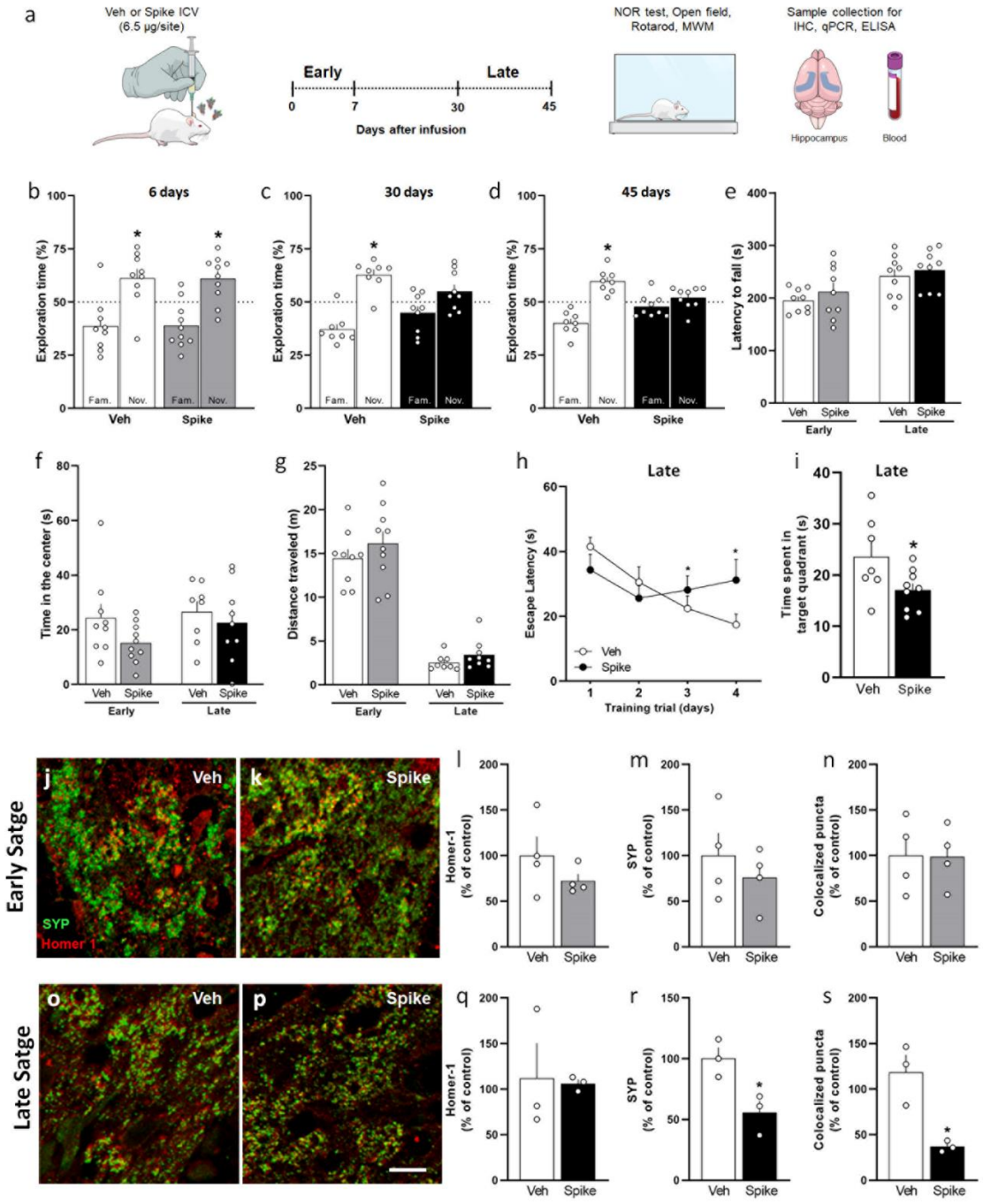

Figure 1 Spike protein causes synapse damage and memory impairment in mice. a, Mice received an i.c.v. infusion of 6,5 µg of SARS-CoV-2 spike protein (Spike), or vehicle (Veh), and were evaluated at early (up to 7 days) or late time points (from 30 to 45 days) after the infusion using behavioral and molecular approaches. **b-d**, Mice were tested in the novel object recognition (NOR) test at 6 days (**b** t=2.626, **p* = 0.0304 for Veh; and t=3.218, **p* = 0.0104, for Spike), 30 days (**c** t=5.099, **p* =0.0014 for Veh), and 45 days after protein infusion (**d** t=5,122, **p* = 0.0014, for Veh); one-sample Student's *t*-test compared to the chance level of 50% (*N* = 8-10 mice per group). **e,** Mice were tested in the Rotarod task at early and late (*N* = 9 mice per group). **f,** Time spent at the center

bioRxiv preprint doi: https://doi.org/10.1101/2022.06.07.495149; this version posted June 8, 2022. The copyright holder for this preprint (which was not certified by peer review) is the author/funder, who has granted bioRxiv a license to display the preprint in perpetuity. It is made available under aCC-BY-ND 4.0 International license.

of the open field arena at early or late stages of the model (*N* = 8-10 mice per group). **g,** Total distance traveled of the open field arena at early or late (*N* = 8-10 mice per group). **h, i,** Escape latencies across 4 consecutive training trials (**h**) and time spent in the target quadrant during the probe trial (**i**) of the MWM test performed at the late stage (**h** $F_{(3, 45)}$ = 2.857, **p* = 0.0475, repeated measures ANOVA followed by Tukey's test; **i** t = 2.211, **p* = 0.0442, Student's *t*-test; *N* = 7-9 mice per group). Representative images of the DG hippocampal region of Veh- (**j, o**) or Spike-infused mice (**k, p**) in the early (**j, k**) and late (**o, p**) stages of the model, immunolabeled for Homer1 (red) and synaptophysin (SYP; green). (**l-n**, **g-s**) Number of puncta for Homer-1 (**l, q**), SYP (**m, r**), and colocalized Homer-1/SYP puncta (**n, s**) in the early (**l-n**) and late (**q-s**) stages of the model. (**r** t = 3.400, **p* = 0.0273; **s** t = 4.204, **p* = 0.0137, Student's *t*-test; *N* = 3-4 mice per group). Scale bar = 20 µm. Symbols represent individual mice. Bars (**b-g**; **i**; **l-n; q-s**) or points (**h**) represent means ± SEM. OD: optical density; IHC: immunohistochemistry; NOR: Novel object recognition.

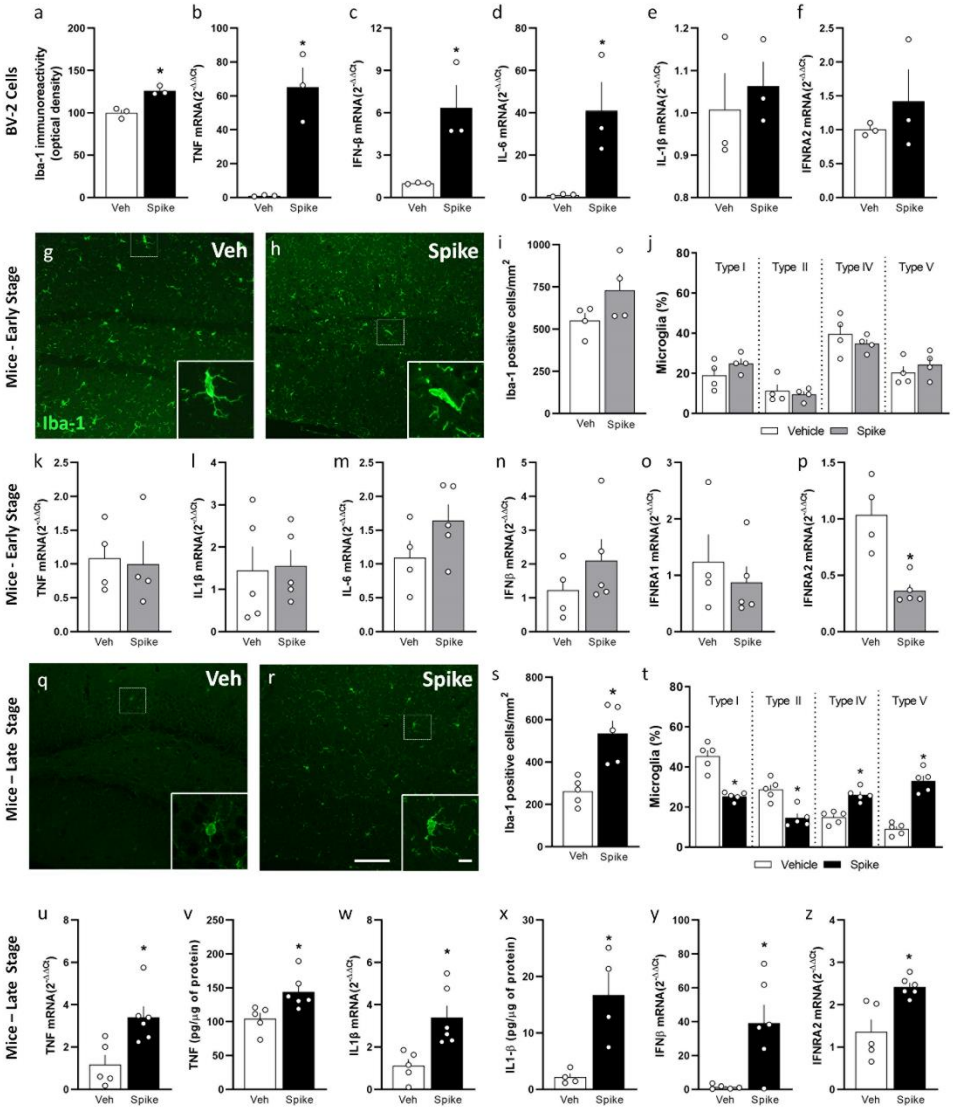

Figure 2 Spike protein induces cytokine upregulation in cultured microglia and triggers delayed brain inflammation and microgliosis in mice. a-f, BV2 cells were treated with SARS-CoV-2 spike protein (Spike) or vehicle (Veh) during 24h, and analyzed by immunocytochemistry or qPCR. Iba-1 immunoreactivity (**a** t=5.567,

bioRxiv preprint doi: https://doi.org/10.1101/2022.06.07.495149; this version posted June 8, 2022. The copyright holder for this preprint (which was not certified by peer review) is the author/funder, who has granted bioRxiv a license to display the preprint in perpetuity. It is made available under aCC-BY-ND 4.0 International license.

*p = 0.0051), mRNA levels of TNF (**b** t=5.557, *p = 0.0051), IFN-β (**c** t=3.307, *p = 0.0297), IL-6 (**d** t=2.968, *p = 0.0412), IL-1β (**e**), and IFNAR2 (**f**); Student's *t*-test; *N* = 3. **g-z,** Mice received an i.c.v. infusion of 6,5 µg of Spike or vehicle (Veh), and were evaluated at early (**g-p**, 3 days) or late time points (**q-r**, 45 days). Representative images of Iba-1 immunostaining in the DG hippocampal region of Veh- (**g, q**) or Spike-infused mice (**h, r**) in the early (**g, h**) and late (**q, r**) stages of the model. Scale bar = 25 µm, inset scale bar = 10 µm. **i, s,** Iba-1 positive cells in the hippocampi of Veh- or Spike-infused mice in the early (**i**) and late (**s** t = 4.086; *p = 0.0035, Student's *t*-test) stages of the model (*N* = 4-5 mice per group). **j, t,** Quantifications of the proportion of each Iba-1-positive cells morphological type in Veh- or Spike-infused mice evaluated in the in the early and late (**t** t = 6.388; *p= 0.0002 for Type I; t = 4.458; *p = 0.0021 for Type II; t =5.513; *p =0.0006 for Type IV; t = 8.384; *p < 0.0001 for Type V, Student's *t*-test) stages of the model (*N* = 4-5 mice per group). **k-p,** qPCR analysis of indicated mRNA isolated from the hippocampus in the early stage of the model. IFNRA2 (**p** t=4.413, *p = 0.0031) (*N* = 4-5 mice per group). **u-z,** Hippocampal proinflammatory mediators in Veh- or Spike-infused mice in the late stage of the model. TNF mRNA (**u** t=3.189; *p = 0.0110) and protein (**v** t=2.885; *p =0.0180) levels. IL-1β mRNA (**w** t=3.322; *p = 0.0089) and protein (**x** t=3.583; *p =0.0116) levels. **y-z** mRNA levels of IFN-β (**y** t=3.713, *p =0.013) and IFNAR2 (**z** t=3.743; *p = 0.0046). Student's *t*-test (*N* = 4-6 mice per group). Symbols represent individual mice, and bars represent means ± SEM.

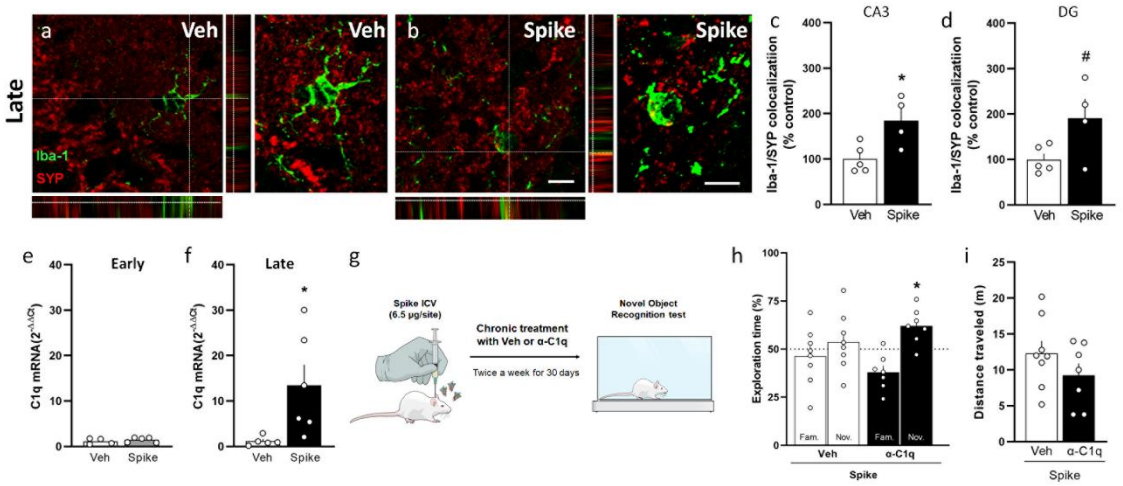

Figure 3: C1q neutralization prevents spike-induced memory impairment in mice. Mice received an i.c.v. infusion of 6,5 µg of SARS-CoV-2 spike protein (Spike), or vehicle (Veh), and were evaluated at early (3 days) or late time points (45 days). **a, b,** Representative images of microglia (Iba-1+, green) engulfing pre-synaptic terminals immunolabeled for synaptophysin (SYP, red) in the DG hippocampal region of Veh- (**a**) or Spike-infused mice (**b**) in the late stage of the model. Scale bar = 25 µm, inset scale bar = 10 µm. **c, d,** Quantification of microglia-SYP colocalization in CA3 (**c** t = 2.949, *p = 0.0214), and DG (**d** t = 2.271, #p = 0.0574) hippocampal regions. Student's *t*-test; (*N* = 4-5 mice per group). **e, f,** C1q mRNA expression in hippocampi of Veh- or Spike-infused mice at early (**e**) or late time points (**f** t = 2.425, *p = 0.0383, Student's *t*-test; (*N* = 4-6 mice per group). **g,** Mice received an i.c.v. infusion of 6,5 µg of Spike, were treated with Veh or 0.3 µg anti-C1q antibody (α-C1q; i.c.v., twice a week, for 30 days), followed by novel object recognition (NOR) testing (**h** t=3.438, *p = 0.0138 for Spike/α-C1q; one-sample Student's *t*-test compared to the chance level of 50%). **i,** Total distance traveled of the open field arena at late (*N* = 7-8 mice per group).

bioRxiv preprint doi: https://doi.org/10.1101/2022.06.07.495149; this version posted June 8, 2022. The copyright holder for this preprint (which was not certified by peer review) is the author/funder, who has granted bioRxiv a license to display the preprint in perpetuity. It is made available under aCC-BY-ND 4.0 International license.

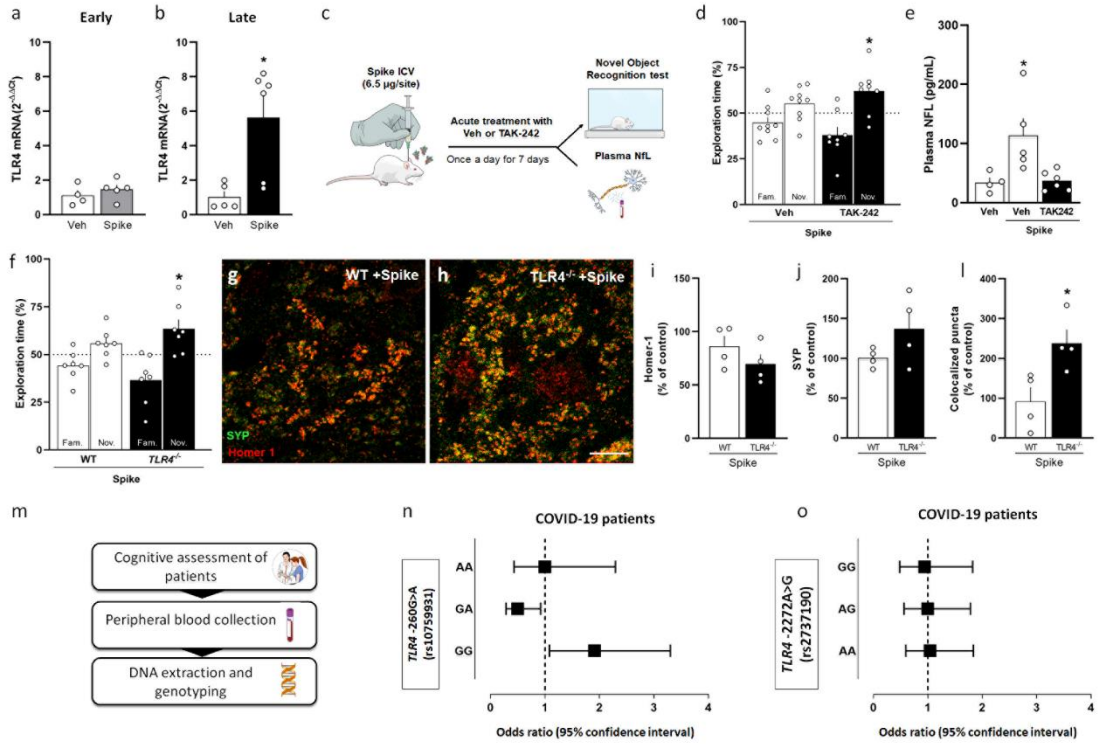

Figure 4: TLR4 mediates spike-induced memory impairment in mice and is associated with post-COVID cognitive impairment in a human cohort. a, b, Mice received an i.c.v. infusion of 6,5 µg of SARS-CoV-2 spike protein (Spike), or vehicle (Veh), and TLR4 mRNA levels in the hippocampi of Veh- or Spike-infused mice were evaluated at early (**a**; 3 days) or late (**b,** 45 days, t = 3.229, **p* = 0.0103, Student's *t*-test) time points (*N* = 4-6 mice per group). **c,** Swiss mice received an i.c.v. infusion of 6,5 µg of Spike and were treated with Veh or the TLR4 antagonist TAK-242 (2 mg/kg, once daily for 7 days, i.p.), and were tested in the late stage of the model in the novel object recognition (NOR) test (**d** t = 2.713, **p* = 0.0301 for Spike/TAK-242; one-sample Student's *t*-test compared to the chance level of 50%, *N* = 8-9 mice per group). **e** Plasma NfL levels evaluated in the late stage of the Spike infusion model (F = 6.329, **p* = 0.0133, one-way ANOVA test, followed by Tukey's test (*N* = 4-6 mice per group). **f,** Wild-type (WT) and TLR4 knockout (*TLR4*$^{-/-}$) mice received an icv infusion of 6,5 µg of SARS-CoV-2 spike protein (Spike) and were tested in the novel object recognition (NOR) test in the late stage of the model (**f** t = 2.744, **p* = 0.0336). One-sample Student's *t*-test compared to the chance level of 50%, *N* = 7 mice per group). **g, h,** Representative images of the DG hippocampal region of WT/Spike (**g**) or *TLR4*$^{-/-}$/Spike (**h**) mice immunolabeled for Homer1 (red) and synaptophysin (SYP; green). Number of puncta for Homer-1 (**i**), SYP (**j**), and colocalized Homer-1/SYP puncta (**l** t = 2.945, **p* = 0.0258; Student's *t*-test; *N* = 4 mice per group). Scale bar = 20 µm. Symbols represent individual mice, and bars represent means ± SEM. **m,** Pipeline to analyze the impact of *TLR4* variants in cognitive status of Post-COVID patients. **n, o,** Forest plots showing odds ratio and 95% confidence interval for risk of cognitive impairment post-COVID-19 by genotype for SNPs *TLR4* -2604G>A (rs10759931; **n**) and *TLR4* −2272A>G (rs2737190; **o**). Each square represents the odds ratio for each genotype, and each horizontal line shows the 95% confidence interval.